THE JOURNAL OF BIOLOGICAL CHEMISTRY VOL. 291, NO. 14, pp. 7357–7372, April 1, 2016

Oxygen-dependent Regulation of Erythropoietin Receptor Turnover and Signaling*

Received for publication, September 28, 2015, and in revised form, February 1, 2016 Published, JBC Papers in Press, February 4, 2016, DOI 10.1074/jbc.M115.694562

Pardeep Heir[‡], Tharan Srikumar[§], George Bikopoulos[‡], Severa Bunda[‡], Betty P. Poon[‡¶], Jeffrey E. Lee[‡], Brian Raught[§], and Michael Ohh[‡¶1]

From the Departments of [‡]Laboratory Medicine and Pathobiology and [¶]Biochemistry, University of Toronto, Toronto, Ontario M5S 1A8 and the [§]Princess Margaret Cancer Centre, Toronto, Ontario M5G 1L7, Canada,

von Hippel-Lindau (VHL) disease is a rare familial cancer predisposition syndrome caused by a loss or mutation in a single gene, *VHL*, but it exhibits a wide phenotypic variability that can be categorized into distinct subtypes. The phenotypic variability has been largely argued to be attributable to the extent of deregulation of the α subunit of hypoxia-inducible factor α, a well established target of VHL E3 ubiquitin ligase, ECV (Elongins/Cul2/VHL). Here, we show that erythropoietin receptor (EPOR) is hydroxylated on proline 419 and 426 via prolyl hydroxylase 3. EPOR hydroxylation is required for binding to the β domain of VHL and polyubiquitylation via ECV, leading to increased EPOR turnover. In addition, several type-specific VHL disease-causing mutants, including those that have retained proper binding and regulation of hypoxia-inducible factor α, showed a severe defect in binding prolyl hydroxylated EPOR peptides. These results identify EPOR as the second *bona fide* hydroxylation-dependent substrate of VHL that potentially influences oxygen homeostasis and contributes to the complex genotype-phenotype correlation in VHL disease.

von Hippel-Lindau (VHL)[2] disease is a rare familial cancer predisposition syndrome characterized by the development of tumors in several organ systems, including the central nervous system and retinal hemangioblastoma (HAB), which represent the two cardinal features of VHL disease, as well as endolymphatic sac tumor of the inner ear, pancreatic cystadenoma, benign cystadenoma of epididymis, adnexal papillary cystadenoma of probable mesonephric origin, clear-cell renal cell carcinoma (RCC), paragangliomas, and pheochromocytoma (PHEO) (1). Some VHL patients also develop polycythemia with or without the other stigmata of VHL disease. VHL disease is subcategorized into type 1, characterized by HAB and RCC without PHEO; type 2A, characterized by PHEO and HAB without RCC; type 2B, characterized by PHEO and HAB with RCC; type 2C, characterized by exclusive development of PHEO; and type 3, which is characterized by the development of polycythemia without an increased cancer predisposition (2). Notably, despite the phenotypic heterogeneity, VHL disease is caused by a mutation or loss of a single gene, *VHL*.

VHL is the substrate recognizing subunit of a multiprotein E3 ubiquitin ligase ECV (Elongins BC/Cul2/VHL) that targets the α subunit of hypoxia-inducible factor (HIFα) for ubiquitylation under normal oxygen tension (3). HIFα is hydroxylated on conserved prolines within the oxygen-dependent degradation domain (ODD) by a family of prolyl hydroxylase enzymes (PHD1–3) in the presence of 2-oxoglutarate, iron, and oxygen (4–7). VHL binds exclusively to prolyl hydroxylated HIFα. Thus, under hypoxia, the unmodified HIFα escapes the recognition by VHL and heterodimerizes with the constitutively expressed HIFβ to form an active transcription factor, which transactivates numerous hypoxia-inducible genes involved in various adaptive processes to hypoxia such as anaerobic metabolism, angiogenesis, and erythropoiesis (8).

Considering the wide phenotypic variability in VHL disease, a prediction was that ECV had more than one substrate. Over the past few years, several proteins have been reported to be substrates of ECV or VHL-associated proteins, such as RBP1 (9), aPKC (10), SPRY2 (11), and β2AR (12). However, the biological or pathophysiological significance in the context of VHL disease of such interactions has remained largely unclear. In contrast, studies have suggested that HIFα deregulation upon VHL mutation or loss contributes to the development of VHL disease in particular HAB and RCC but did not seem to be involved in the development of PHEO (13, 14). Intriguingly, binding to extracellular matrix protein fibronectin was lost in all disease-causing VHL mutants tested to date (15). However, the biological significance of this lost interaction or its contribution, if any, to genotype-phenotype correlation in VHL disease remains unanswered.

Erythropoietin (EPO) is a glycoprotein hormone whose gene is transactivated by HIF2α (16–21). EPO binds to EPO receptor (EPOR) expressed on erythroid progenitor cells to initiate JAK2-STAT5 signal transduction cascade that promotes a surge of proliferation followed by terminal differentiation into mature oxygen-carrying red blood cells (22, 23). Truncation mutations in EPOR that lead to a failure in negative regulation or JAK2 mutations that cause increased activity are often found in primary form of polycythemia, which are instigated by an exaggerated response to EPO stimulus (24–26). In this regard,

* This work was supported by funds from the Canadian Institutes of Health Research. The authors declare that they have no conflicts of interest with the contents of this article.

[1] To whom correspondence should be addressed: Dept. of Laboratory Medicine and Pathobiology, Dept. of Biochemistry, University of Toronto, 1 King's College Circle, Toronto, ON M5S 1A8, Canada. Tel.: 416-946-7922; Fax: 416-978-5959; E-mail: michael.ohh@utoronto.ca.

[2] The abbreviations used are: VHL, von Hippel-Lindau; HAB, hemangioblastoma; HIF, hypoxia-inducible factor; EPO, erythropoietin; EPOR, EPO receptor; PHD, prolyl hydroxylase; RCC, renal cell carcinoma; PHEO, pheochromocytoma; ODD, oxygen-dependent degradation domain; EloB/C, elongin B/C; Ni-NTA, nickel-nitrilotriacetic acid; α-MEM, α-minimal essential medium; MEF, mouse embryonic fibroblast; VBC, VHL, elongin B, and elongin C.

it is noteworthy that primary polycythemia patients often have a reduced serum EPO level.

Mutations in HIF2α have been identified in the vicinity of its conserved prolyl residue, Pro^{531}, in several polycythemia patients (27). Some of these mutations cause a reduction in binding to and catalysis by PHD enzymes, as well as a defect in binding to VHL (28). Mutations in PHD2 have also been identified, which cause erythrocytosis in a HIF2α-dependent manner (27, 29). These patients have elevated or higher than the expected serum EPO levels. Consistent with these observations, *PHD2* knock-out mice develop secondary polycythemia with high serum EPO level (30, 31). In contrast, *PHD1* and *PHD3* double knock-out mice develop polycythemia but curiously without an increased serum EPO level (30), suggesting a yet undefined HIF2α-independent mechanism. Notably, anemia in rats has been shown to increase the number of cell surface EPOR (32).

Here, we show for the first time that EPOR turnover is regulated by oxygen tension. The conserved prolyl residues within the cytoplasmic region of EPOR become hydroxylated by PHD3, a process that is strictly dependent on oxygen, and targeted for ubiquitylation via ECV. Molecular knockdown or knock-out of PHD3 or VHL promoted EPOR expression level and EPO-dependent downstream signaling. Moreover, myeloid colony formation and signal transduction were accentuated by hypoxia. Notably, several type-specific VHL mutants, some of which retained proper binding and regulation of HIFα, showed a profound defect in binding synthetically hydroxylated EPOR peptide. These findings reveal EPOR as a potential substrate of VHL tumor suppressor complex that may contribute to the phenotypic spectrum of VHL disease.

Experimental Procedures

Cells—786-O, HEK293A, and HEK293T cells (American Type Culture Collection) were maintained in Dulbecco's modified Eagle's medium (Invitrogen) supplemented with 10% heat-inactivated fetal bovine serum (Wisent) at 37 °C in a humidified atmosphere with 5% CO_2. 786-O lines stably expressing HA-VHL or empty plasmid were previously described (3, 4). γ2A cells were a kind gift from Dr. George Stark (Cleveland Clinic) and were maintained in DMEM supplemented with 10% heat-inactivated fetal bovine serum, 1 mM sodium pyruvate, and 0.4 mg/ml G418 (Sigma). Ba/F3 cells were maintained in RPMI medium supplemented with 10% heat-inactivated fetal bovine serum and 100 pg/ml IL-3, whereas Ba/F3-EPOR cells were maintained using 0.5 unit/ml EPO (Janssen Inc.) instead as previously described (33). UT-7 cells (Leibniz Institut-Deutsche Sammlung von Mikroorganismen und Zellkulturen) were maintained in α-MEM (Invitrogen) supplemented with 20% premium heat-inactivated fetal bovine serum (Wisent) and 5 ng/ml GM-CSF (Invitrogen).

Antibodies—The following antibodies were obtained from Santa Cruz Biotechnology: pEPOR (sc-20236-R), EPOR (sc-697), elongin B (sc-11447), IL-3Rα (sc-681), βc (sc-678), and GAL4 (sc-510). The following antibodies were obtained from Cell Signaling Technology: JAK2 (3230), pJAK2 (3771), HA (3724), VHL (2738), and pSTAT5 (9314). The following antibodies were obtained from Sigma: vinculin (V9264), β-actin (A5316), tubulin (T6074), and FLAG-M2 (F1804). The following antibodies were obtained from Novus Biologicals: HIF2α (NB100-122), FLAG (NB100-63146), and PHD3 (NB100-303). Anti-EPOR (ab10653) antibody was obtained from AbCam, whereas anti-EPOR (MAB307) antibody was obtained from R&D Systems. Antibodies used to detect HIF1α (610958) and VHL (556347) were obtained from BD Biosciences. Anti-HA (12CA5), anti-CUL2 (51-1800), anti-STAT5 (06-553), and anti-ubiquitin (Z0458) antibodies were obtained from Boehringer Ingelheim, Invitrogen, Upstate, and Dako, respectively.

Chemicals and Reagents—Dimethyloxalylglycine was purchased from Frontier Scientific. Cycloheximide (C4859) and cobalt chloride were obtained from Sigma. MG132 (IZL-3175-v) was obtained from Peptides International. Streptavidin-agarose resin was obtained from Thermo Scientific. HA-ubiquitin was purchased from Boston Biochem. The cell surface biotinylation was performed using EZ-Link Sulfo-NHS-LC-Biotin (Thermo) in accordance with the manufacturer's instructions.

Plasmids—Human EPOR cDNA was provided by Dr. William Y. Kim, and murine EPOR was provided by Dr. Dwayne Barber, which were subcloned into pCMV6 to integrate a C-terminal Myc-FLAG tag. Where viruses were used to infect cells with EPOR-FLAG, it was subcloned from the above plasmids and inserted into pLenti-CMV-GFP-Hygro (Addgene: 17446 (34)) by replacing GFP. The same strategy was used for HA-VHL. Untagged elongin B/C (EloB/C) was previously cloned into a pACYCDuet-1 vector (gift from the Structural Genomics Consortium, Oxford, UK). The following plasmids were generated using the indicated tagged vectors, and the inserts were generated using standard PCR: pcDNA3-FLAG-muCytoEPOR, pcDNA3–3×FLAG-huCytoEPOR, pcDNA3-SBP-CytoEPOR, pcDNA3-GAL4-HA-PEP6, pET-15b-(His)-CytoEPOR, pGEX-4T-1-(GST)-PHD3, and pGEX-4T-1-(GST)-VHL_{19}. Overlap extension was used to generate GAL4-HA-PEP6(AAAAAA). HA-VHL, HA-VHL(63–155), HA-VHL(156–213), HA-VHL(Y112N), HA-VHL(D121G), HA-VHL(Y98H), HA-VHL(Y112H), HA-VHL(A149T), HA-VHL(R64P), HA-VHL(V84L), HA-VHL(F119S), HA-VHL(K159E), and HA-VHL(L188V) plasmids have previously been described (3, 14). HA-PHD1, HA-PHD2, HA-PHD3, and HA-PHD3(H196A) plasmids were obtained from Addgene (18961, 18963, 18960, and 22717 (35)). psPAX2 and pMDG1.vsvg were a kind gift from Linda Z. Penn. The following pGIPZ-based shRNA plasmids were purchased from Thermo Scientific: shPHD3 (V3LMM_440956), shPHD3 (V3LHS_414249), shVHL (V2LHS_202399), and pGIPZ control (RHS4346).

CRISPR/Cas9-mediated Gene Editing—pLentiCRISPR (49535) (36) was obtained from Addgene, and the following sequences derived from exon 1 of the indicated genes were used to create guides: PHD3, 5′-CACGTGGATCGGGGGC-AACG; and VHL, 5′-CCCGTATGGCTCAACTTCGA. The cells were infected with lentivirus as described below.

Peptides—The following peptides containing an N-terminal Biotin-Ahx-KKK motif and C-terminal amidation were synthesized by Genscript where (Hyp) denotes hydroxyproline: PEP6, LCPELPPTPPHLKYL; PEP6-Pro^{419}-OH, LC(Hyp)ELPPTP-

PHLKYL; PEP6-Pro^{425}-OH:LCPELPPT(Hyp)PHLKYL; and PEP6-Pro^{426}-OH, LCPELPPTP(Hyp)HLKYL. The recentered peptides were as follows: Pro^{419}, RPWTLCPELPPTPPH; Pro^{419}-OH, :RPWTLC(Hyp)ELPPTPPH; Pro^{419}-OH,Pro^{426}-OH, RPWTLC(Hyp)ELPPTP(Hyp)H; and Pro^{419},Pro^{426}-OH, RPWTLCPELPPTP(Hyp)H. ODD and ODD-OH peptides (HIF1α Pro^{564}-OH) have been described previously (4).

Immunoblotting and Immunoprecipitation—Cells were harvested in modified radioimmunoprecipitation assay buffer (50 mM Tris, pH 8, 150 mM NaCl, 1% Triton X-100, 0.5% sodium deoxycholate, 0.1% SDS) supplemented with protease inhibitors (Roche) and, when required, phosphatase inhibitors (Roche). Experiments requiring immunoprecipitation were lysed in EBC lysis buffer (50 mM Tris, pH 8, 120 mM NaCl, 0.5% Nonidet P-40) supplemented with protease inhibitors and phosphatase inhibitors when needed. Lysates were immunoprecipitated using the indicated antibodies along with protein A-Sepharose (Repligen). Bound proteins were washed five times in NETN buffer (20 mM Tris, pH 8, 100 mM NaCl, 1 mM EDTA, 0.5% Nonidet P-40) and eluted by boiling in sample buffer. Proteins were resolved by SDS-PAGE, electrotransferred onto PVDF membrane (Bio-Rad), blocked, and probed with the antibodies indicated in the figures.

Lentiviral Production and Infection of Cell Lines—HEK293T cells were transfected with psPAX2, pMDG1.vsvg, and either a pGIPZ, pLenti-CMV-GFP-Hygro, or pLentiCRISPR transfer vector. Lentivirus containing supernatant was collected at 48 and 72 h post-transfection. Lentiviral supernatant was filtered and applied to the indicated cell lines. UT-7 cells required the addition of 4 μg/ml Polybrene (Millipore) and GM-CSF at a final concentration of 5 ng/ml. Selection was started 24 h after infection using puromycin (2 μg/ml) or hygromycin (250 μg/ml) (both from Wisent). Note that polyclonal populations were generated and used for experiments, except for knock-out cells for which monoclonal cell lines were generated.

Protein Purification—pGEX-4T-1-PHD3 (or empty pGEX-4T-1 for GST control protein) was expressed in BL21 *Escherichia coli* and induced with 0.1 mM isopropyl-β-D-thiogalactopyranoside (Sigma) overnight. Bacterial pellets were lysed in PBS supplemented with protease inhibitors (Roche), sonicated, cleared, and bound to glutathione-Sepharose (GE Healthcare). The beads were washed and GST-PHD3 was eluted using GST elution buffer (50 mM Tris, pH 8, 30 mM glutathione). pET15-huCytoEPOR was expressed in Rosetta-2 and induced with 0.1 mM isopropyl-β-D-thiogalactopyranoside overnight. Bacterial pellets were lysed in 50 mM Tris, pH 8, 300 mM NaCl, 20 mM imidazole supplemented with protease inhibitors; sonicated; cleared; and bound to Ni-NTA-agarose (Invitrogen). Beads were washed and eluted using an imidazole gradient.

VHL_{19} was co-expressed with EloB/C in *E. coli* BL21 (DE3). The cell cultures were grown to $A_{600} = 0.6$ and induced with a final concentration of 1 mM isopropyl-β-D-thiogalactopyranoside for 5 h at 37 °C. The cells were subsequently resuspended in Buffer A (5 mM HEPES, pH 7.4, 200 mM NaCl, and 1 mM DTT) supplemented with 1× Complete EDTA-free protease inhibitor (Roche) and lysed using a Constant Systems cell disruption system (30 kpsi). The lysate was then briefly sonicated on ice for 30 s, and the cellular debris was removed by centrifugation at 34,000 × *g* for 40 min prior to loading onto a glutathione-Sepharose column (GE Healthcare). The VHL-EloB/C complex was eluted in Buffer A with 10 mM reduced glutathione and treated with thrombin (Millipore; 1 unit/mg of protein) at 4 °C overnight to remove the GST fusion protein. The complex was dialyzed overnight in buffer A prior to purification on a preparation grade Superdex 200 10/300 column. The peak corresponding to the 1:1:1 VHL-EloB/C complex (44.1 kDa) was collected.

Biolayer Interferometry—Biotinylated EPOR and HIF1α ODD peptides were synthesized (Genscript), diluted to 100 μg/ml in BLI kinetics buffer (buffer A, 0.5% (w/v) BSA and 0.02% (v/v) Tween 20), and immobilized over 120 s onto a streptavidin-coated BLI biosensor (Pall Corp). The purified 1:1:1 VHL-EloB/C ternary complex was diluted in BLI kinetics buffer over various protein concentrations, and its association to the immobilized peptide was measured over 120 s. Subsequently, the biosensor was immersed into BLI kinetics buffer over 180 s to dissociate the VHL-EloB/C-peptide complex. The kinetic parameters (K_d, k_a, and k_d) were calculated from the sensorgrams using the BLItz Pro software (version 1.1.0.16).

In Vitro Binding Assays—Purified proteins were incubated in a final reaction volume of 30 μl of EBC at 30 °C. After 1 h of incubation, 1 ml of EBC buffer was added along with Ni-NTA, and the mixture was rocked at 4 °C for 1 h. Bound proteins were washed five times prior to elution by boiling in sample buffer. Proteins were visualized by staining with GelCode (Thermo). Binding assays using biotinylated peptides were performed as previously described (37) with the following modifications: methionine was not radiolabeled, so immunoblotting was used to detect rabbit reticulocyte *in vitro* translated (Promega) proteins; EBC buffer was supplemented with 1 mM DTT; washes were conducted in NETN containing 300 mM NaCl instead of 100 mM NaCl.

In Vitro Hydroxylation—*In vitro* hydroxylation assays were performed essentially as previously described (37). 1 μg of the indicated peptide was attached onto 30 μl of streptavidin-agarose slurry. The final reaction volume was 200 μl, consisting of 1× PHA (40 mM HEPES, pH 7.4, 80 mM KCl), 100 μM $FeCl_2$, 2 mM ascorbate, 5 mM 2-oxoglutarate, and 10 μl of programmed reticulocyte lysate. The reaction was incubated at room temperature for 2 h. Where purified components were used, 2 μg of His-CytoEPOR was used and 1 μg of GST-PHD3.

Competition Assay—HEK293 cells were transfected with VHL and substrate. The complex was affinity-purified and separated into four tubes each with an equivalent quantity of beads, the indicated amount of peptide (0–6 μg), and EBC lysis buffer up to 100 μl. The tubes were incubated at 30 °C for 30 min with mixing every 5 min. Next, 1 ml of EBC was added, and the tubes were rocked at 4 °C for 1 h. The beads were washed in NETN, and proteins were eluted by boiling in sample buffer.

Ubiquitylation Assays—*In vitro* ubiquitylation assay was performed using S100 fractions as described previously (3). For *in vivo* ubiquitylation, UT-7 cells were treated with 10 μM MG132 for 4 h. The cells were lysed in EBC lysis buffer supplemented with 2% SDS and boiled for 15 min to denature proteins and eliminate protein interactions. The supernatant was collected

and diluted so the final concentration of SDS would be less than 0.1%, and immunoprecipitation was performed.

Dot Blot—Peptides were spotted onto PVDF membrane (Bio-Rad). The membrane was blocked in TBST (100 mM Tris, 150 mM NaCl, 0.5% Tween20) containing 4% milk. The membrane was washed and probed using streptavidin-HRP (Cell Signaling Technology).

Quantitative Real Time PCR—RNA was isolated from three biological replicates using the RNeasy mini kit (Qiagen), with an on-column DNase digestion (Qiagen) according to the manufacturer's instructions. First strand cDNA synthesis was performed using SuperScript II reverse transcriptase (Invitrogen). Quantitative real time PCR was performed using SsoAdvanced SYBR Green Supermix (Bio-Rad) and the following primer pairs: EPOR-F, 5′-GAAGTAGTGCTCCTAGACGCC, and EPOR-R, 5′-CCTCGTAGCGGATGTGAGAC or U1snRNP70-F, 5′-GCTCCGGAGAGAGTTTGAGG, and U1snRNP70-R, 5′-TAAGCGGAGTGCATGTCTCG.

Cytokine Stimulation of Cells—Prior to experiments involving cytokine treatment, cells were washed extensively in plain medium and then resuspended in base medium supplemented with 10% fetal bovine serum. The cells were maintained in cytokine free medium overnight. The cells were treated with the indicated cytokine for the indicated period of time. In experiments involving a short dose of EPO treatment to UT-7 cells, plain α-MEM was added to a Falcon tube containing EPO and an equivalent volume of medium as the cells that were starved. The cells were poured into the Falcon tube and inverted to eliminate the slow rate at which diffusion would have occurred.

In Vitro Differentiation of UT-7 Cells—The cells were washed extensively in plain α-MEM and starved overnight in α-MEM supplemented with 20% fetal bovine serum and puromycin and without GM-CSF. The cells were then grown at 7% oxygen tension for 9 days in α-MEM supplemented with 20% fetal bovine serum, puromycin and 1 unit/ml EPO. On the last day, cells were washed in PBS twice and then lysed by vortexing in 3 volumes of lysis solution H (50 mM Tris, pH 7, 25 mM KCl, 5 mM $MgCl_2$, 1 mM β-mercaptoethanol, 0.3% Triton X-100) similar to as previously described (38) and centrifuged on a tabletop centrifuge at 4 °C for 10 min at maximum speed. The supernatant was collected and placed on ice. The total protein concentration was determined using a Bradford assay. The quantity of hemoglobin was determined using a hemoglobin assay kit (Abnova). 50 μl of the above sample was incubated with 200 μl of the reagent provided for 5 min, and the absorbance at 400 nm was read. After determining the concentration of hemoglobin in the sample, the values were normalized to total protein level. The experiment was performed in triplicate or quadruplicate three independent times. UT-7-pGIPZ control cells were arbitrarily set to 10.

Colony Forming Assay—UT-7 cells were cultured in triplicate in Methocult H4230 (Stemcell Technologies) supplemented with 10% heat-inactivated premium FBS (Wisent), α-MEM and EPO where indicated. The cells were maintained in normoxia (21% oxygen) or hypoxia (1% oxygen) for 10 days. Colonies of greater than 30 cells were scored. The experiment was performed three independent times.

Mass Spectrometry—In vitro hydroxylated His-huCytoEPOR was reduced, alkylated, and subjected to proteolysis with LysC for 16 h, followed by V8 for an additional 8 h. The resulting peptides were lyophilyzed and resuspended in 0.1% formic acid. The samples were analyzed on an Orbitrap Velos mass spectrometer in data-dependent mode, where each full MS scan (at 60,000 resolution in the Orbitrap) was followed by up to 20 collision-induced dissociations in the ion trap. The hydroxylated peptides were identified by multiple database search algorithms (Peaks score 40.67, Sequest XCorr 1.27, deltaCN 0.11, MS-Amanda score 33.18, PeptideProphet confidence value of 0.94), with a parent mass error of −1.4 ppm.

Immunofluorescence Microscopy—Cells were grown on coverslips, and 48 h post-transfection they were washed and fixed in cold 100% methanol at −20 °C for 30 min. After an hour of blocking with 1% normal goat serum in PBS, the cells were then incubated for 1 h (at room temperature) with antibodies recognizing calreticulin (Abcam) and FLAG. The cultures were washed and then incubated for an additional 1 h with fluorescein-conjugated goat anti-rabbit FITC (*green*) and goat anti-mouse rhodamine (*red*) secondary antibodies. The nuclei were stained with DAPI (*blue*). Coverslips were mounted on slides with VectaShield mounting medium (Vector Labs). Immunostained cells were visualized with an Axioplan2 imaging microscope (Carl Zeiss) and imaged with an Axiocam HRM digital camera.

Statistical Analysis—The Results are presented as the mean values ± the standard deviation. A Student's *t* test was used to determine the level of statistical significance achieved. Statistical analysis was performed using GraphPad Prism 5.0 software.

Results

Oxygen Promotes EPOR Turnover—We asked whether oxygen influences the EPO-dependent growth of human erythroleukemia UT-7 cells that express endogenous EPOR. The cells were plated for a colony forming assay in semisolid medium containing increasing amounts of EPO and maintained in normoxia or hypoxia. Increased colony formation was observed under hypoxia relative to normoxia (Fig. 1*A*). After validating and optimizing the anti-EPOR antibody (Fig. 1*B*), we asked whether oxygen influences EPOR expression and downstream signaling. UT-7 cells were cytokine-starved and maintained in a gradient of oxygen tension, and then the cells were briefly treated with or without constant concentration of exogenous EPO. Interestingly, oxygen tension was inversely correlated to total EPOR level, whereas the level of total JAK2 remained unchanged (Fig. 1*C*) (note that EPOR presents as variable multiple bands because of glycosylation). As expected, EPO treatment promoted EPOR and downstream JAK2-Tyr^{1007} phosphorylation, but notably, the extent of phosphorylation was markedly elevated under reduced oxygen tension (Fig. 1*C*). However, the level of *EPOR* mRNA remained unchanged irrespective of oxygen tension (Fig. 1, *D* and *E*). The maintenance of mouse embryonic fibroblasts (MEFs) that ectopically express murine EPOR-FLAG and murine pro-B Ba/F3 cells that stably express ectopic EPOR under hypoxia likewise increased EPOR level (Fig. 1, *F* and *G*).

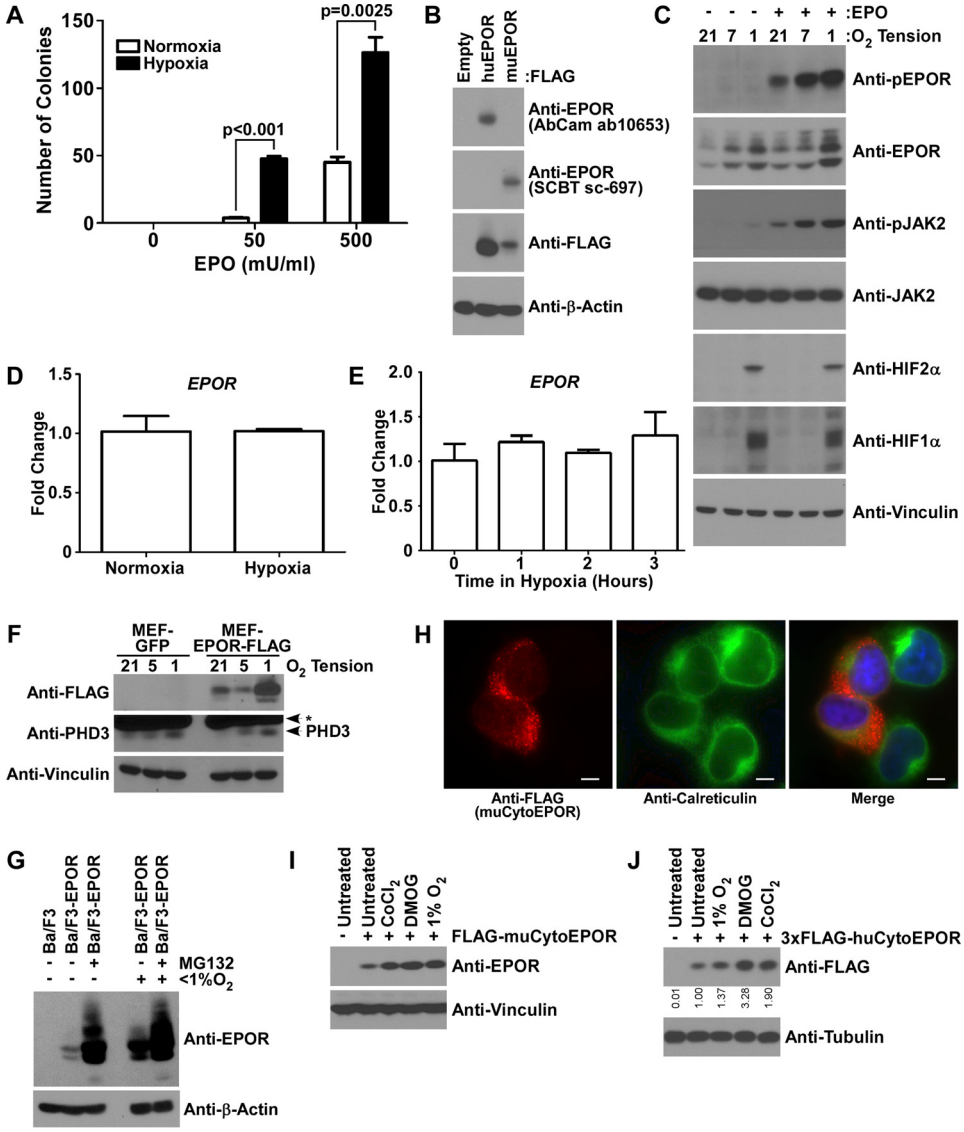

FIGURE 1. **Oxygen influences EPOR stability.** *A*, an equal number of UT-7 cells were plated in triplicate in semisolid medium containing the indicated dosage of EPO. The cells were maintained in normoxia (21% O_2) or hypoxia (1% O_2) for 10 days. Colonies consisting of greater than 30 cells were scored. A Student's *t* test was used to assess the significance. Graphed is a representative result of three independent experiments. *B*, HEK293 cells were transfected with human (*hu*) or murine (*mu*) EPOR. The cells were lysed, resolved by SDS-PAGE, and immunoblotted using the indicated antibodies. *C*, UT-7 cells were maintained in varying levels of hypoxia and deprived of cytokines overnight. The cells were treated with 1 unit/ml EPO for 90 s and lysed, and the indicated proteins were detected by immunoblotting. Presented is a representative of three independent experiments. *D* and *E*, UT-7 cells were cytokine-starved and maintained at ambient oxygen tension or 1% oxygen tension overnight (*D*) or the indicated number of hours (*E*). Total RNA was isolated from three biological replicates, and quantitative real time PCR was performed. Normoxic expression was arbitrarily set to 1. A Student's *t* test determined that the results were not significantly different. *F*, MEF cells were infected with lentivirus encoding GFP or EPOR. The cells were maintained at the indicated oxygen tensions overnight. The cells were lysed, and the indicated proteins were detected by immunoblotting using the indicated antibodies. *G*, Ba/F3 cells were treated with 10 μM MG132 and/or less than 1% oxygen for 5 h. The indicated proteins were detected by immunoblotting. *H*, HEK293 cells were transfected with FLAG-muCytoEPOR. The indicated proteins were visualized by immunofluorescence. *Scale bar*, 10 μm. *I* and *J*, HEK293 cells were transfected with human or mouse CytoEPOR plasmids and plated into a large dish. The cells were split into equivalent smaller plates and treated with 200 μM $CoCl_2$, 1 mM dimethyloxalylglycine (*DMOG*), or hypoxia overnight. Proteins were detected by immunoblotting using the indicated antibodies. Densitometry represents the average value from three independent experiments. * denotes a nonspecific band.

EPOR has previously been reported to undergo endoplasmic reticulum-associated degradation (39). We asked whether the oxygen-dependent regulation of EPOR expression was direct or indirect via endoplasmic reticulum-associated degradation by measuring the steady-state expression level of human (hu) and murine (mu) cytoplasmic EPOR lacking the N-terminal segment containing the ER-targeting sequences in the presence or absence of hypoxia treatment or mimetics. As expected, hu/muCytoEPOR was excluded from the ER as noted by non-overlapping staining pattern with calreticulin and localized in the cytosol (Fig. 1*H*), and its level was increased under hypoxia or in the presence of hypoxia mimetics, cobalt chloride ($CoCl_2$), and dimethyloxalylglycine (Fig. 1, *I* and *J*). These results suggest that the cytoplasmic region contains an element(s) that imparts oxygen-dependent stability of EPOR.

VHL Negatively Regulates EPOR via Ubiquitylation—Considering the pivotal role of VHL in oxygen homeostasis and in the oxygen-dependent recognition of proly hydroxylated substrate HIFα, we asked whether VHL binds to EPOR in an oxygen-dependent manner. Ectopic VHL expressed in HEK293

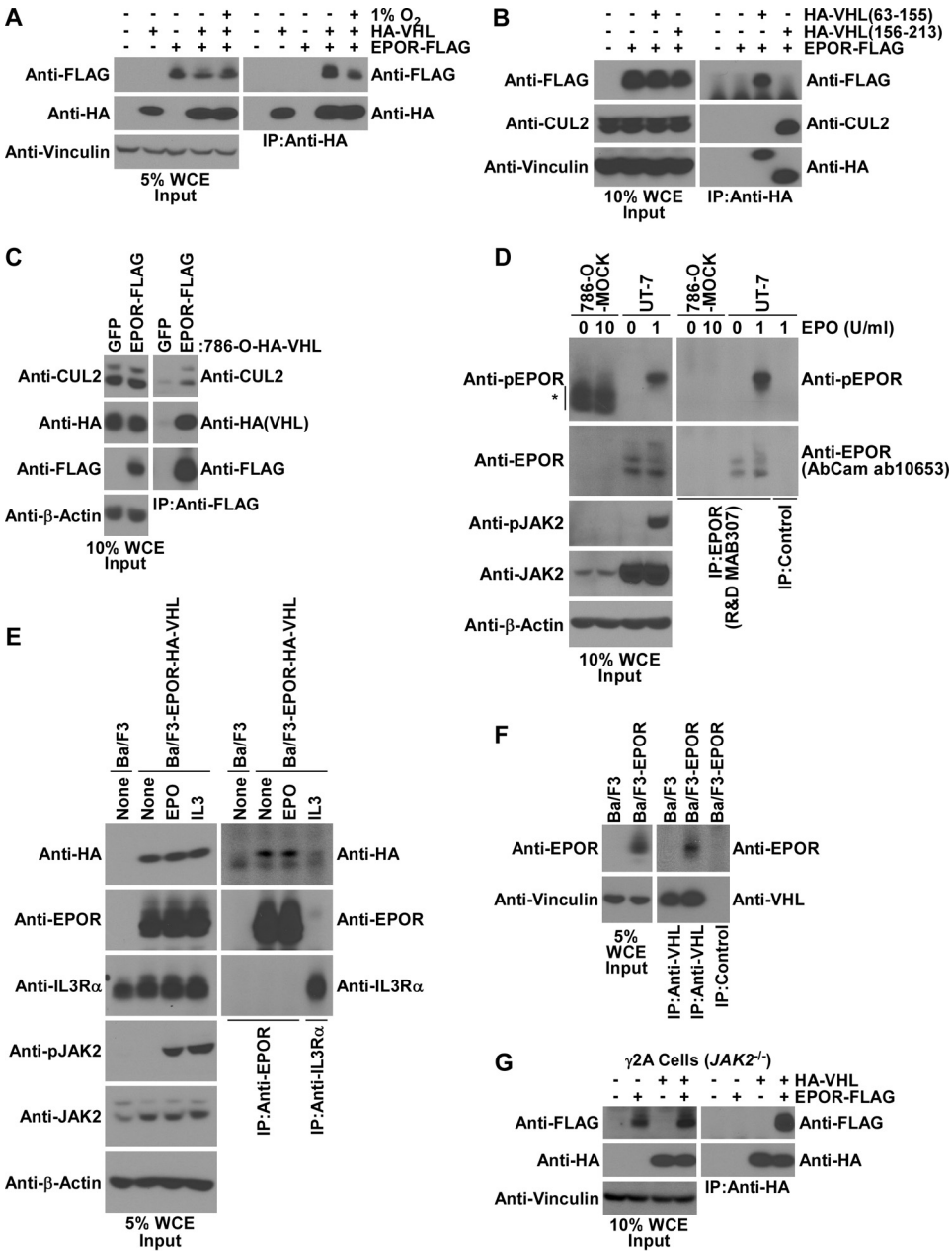

FIGURE 2. **VHL interacts with EPOR.** *A* and *B*, HEK293 cells were transfected with the indicated plasmids and treated with hypoxia where indicated. The cells were treated with 10 μM MG132 for 4 h, lysed, and immunoprecipitated using anti-HA antibody. The proteins were detected by immunoblotting with the indicated antibodies. *C*, 786-O-HA-VHL cells were infected to stably express GFP or EPOR-FLAG. The cells were treated with 10 μM MG132 for 4 h and immunoprecipitated using anti-FLAG antibody. Bound proteins were detected by immunoblotting with the indicated antibodies. *D*, the indicated cell lines were treated with the indicated amount of EPO for 30 min. The cells were lysed, and anti-EPOR or control immunoprecipitation was performed. The proteins were resolved by SDS-PAGE, and immunoblotting was used to detect the indicated proteins. *E*, Ba/F3 cell lines were cytokine-starved overnight. The cells were treated with 10 μM MG132 for 5 h prior to lysis. The cells were treated with the indicated cytokines. The cells were lysed, and immunoprecipitation was performed with the indicated antibodies. Bound proteins were resolved by SDS-PAGE and detected using the indicated antibodies. *F*, Ba/F3 cell lines were treated with 10 μM MG132 for 5 h. The cells were lysed and immunoprecipitated using the indicated antibodies. The bound proteins were resolved by SDS-PAGE and detected using the indicated antibodies. *G*, γ2A cells were transfected with the indicated constructs. The cells were lysed and immunoprecipitated with the indicated antibodies. The bound proteins were resolved by SDS-PAGE and detected using the indicated antibodies. *WCE*, whole cell extract; *IP*, immunoprecipitated. * denotes a nonspecific band. All experiments were performed at least three times.

cells bound to EPOR, but this interaction was diminished under hypoxia (Fig. 2*A*). Similar to HIFα, EPOR bound to the β domain of VHL (residues 63–155), whereas the α domain of VHL (residues 156–213) bound to Cul2, as expected (Fig. 2*B*) (3). In addition, EPOR co-precipitated VHL and Cul2 in VHL-null 786-O renal cell carcinoma cells reconstituted with HA-VHL and infected with lentivirus-EPOR-FLAG (Fig. 2*C*), because 786-O cells do not contain detectable endogenous EPOR (Fig. 2*D*).

β-TrCP and SOCS3 containing cullin-RING E3 ubiquitin ligases have also been shown to associate with EPOR but following EPO stimulation (40–42). We asked whether VHL interacts with EPOR in a cytokine-dependent manner. Ba/F3-EPOR cells stably expressing HA-VHL were cytokine-starved

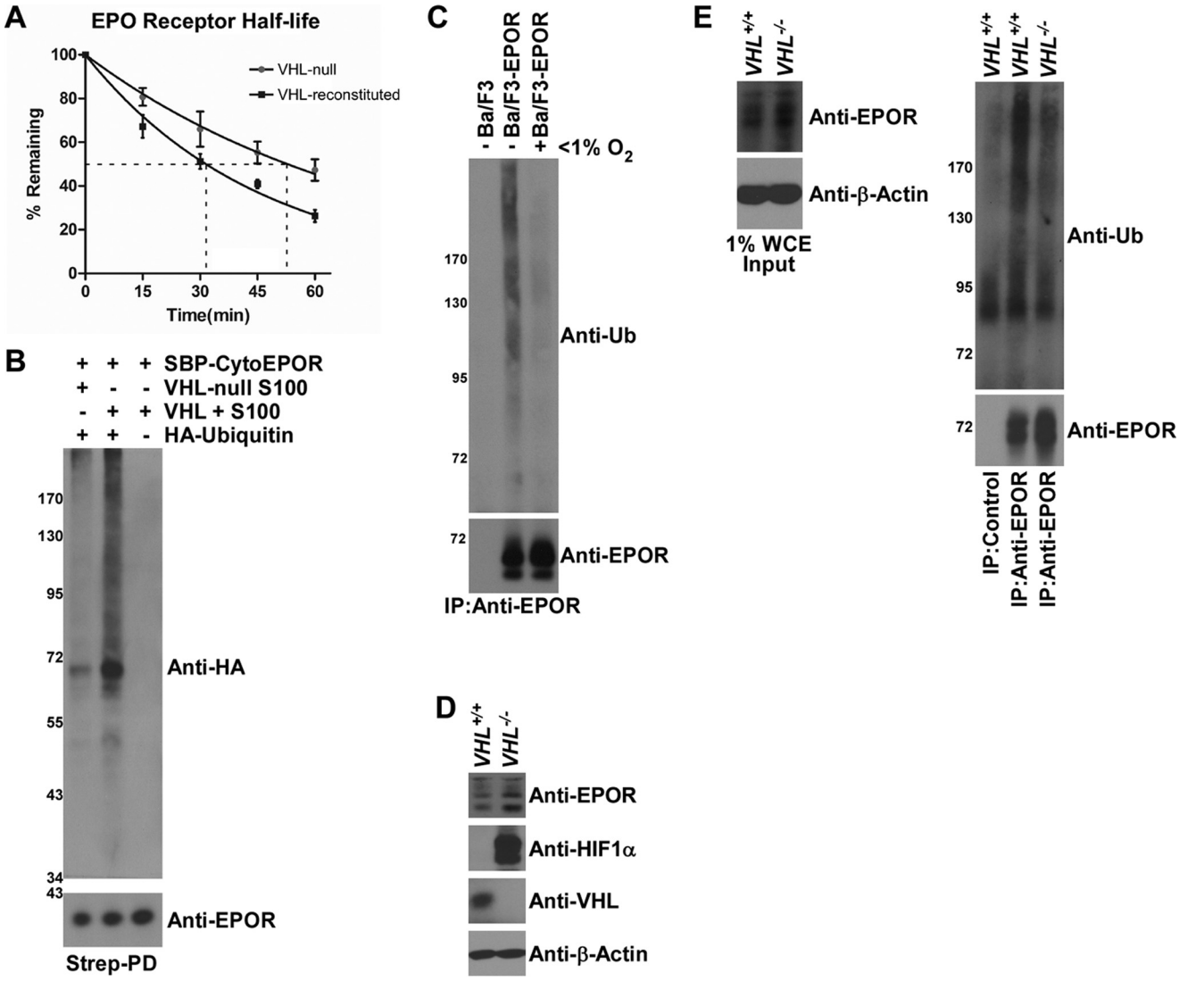

FIGURE 3. **VHL regulates EPOR stability.** *A*, 786-O-Mock and 786-O-HA-VHL cells were infected to stably express EPOR-FLAG. The cells were treated with 50 μg/ml cycloheximide for up to 60 min. EPOR protein levels were detected through anti-FLAG immunoblotting and quantified. The experiment was performed in triplicate, and the mean was plotted. Student's *t* test at 60 min was calculated as $p = 0.0209$. A one-phase decay curve was used to model the amount of EPOR remaining as a function of time. *B*, *in vitro* translated SBP-CytoEPOR was incubated with the indicated S100 fractions in the presence or absence of ubiquitin. A streptavidin pulldown was performed, beads were washed, and bound protein was eluted by boiling in sample buffer. Ubiquitylated species were detected by immunoblotting. *C*, Ba/F3 cells were treated with MG132 and the indicated oxygen tension for 5 h. Anti-EPOR immunoprecipitation was performed, and the indicated proteins were detected by immunoblotting. *D*, UT-7 cells were lysed, and the indicated proteins were detected by immunoblotting to assess for CRISPR-Cas9 mediated gene editing. *E*, parental UT-7 cells or VHL-null UT-7 cells were lysed and boiled in SDS-containing buffer. Endogenous EPOR or control was immunoprecipitated, and ubiquitylated EPOR was detected by immunoblotting. *WCE*, whole cell extract; *IP*, immunoprecipitation; *Strep-PD*, streptavidin pulldown. All experiments were performed at least three times.

and then treated with MG132 and EPO. VHL bound to EPOR, but not IL-3 receptor, irrespective of cytokine stimulation (Fig. 2, *E* and *F*). JAK2 has been reported previously to assist in EPOR trafficking to the plasma membrane (43). We asked whether JAK2 is necessary for the interaction between EPOR and VHL and observed that ectopic VHL bound to EPOR in γ2A cells, which are devoid of JAK2 (Fig. 2*G*). These results suggest that JAK2 and EPO stimulation is not required for the binding between VHL and EPOR.

EPOR half-life increased from ~30 to 50 min in 786-O cells devoid of VHL in comparison to isogenically matched VHL-reconstituted cells ($p = 0.0209$; Fig. 3*A*). We next asked whether the increased rate of EPOR turnover was due, at least in part, to VHL-mediated ubiquitylation. CytoEPOR polyubiquitylation was observed using VHL-reconstituted S100 cellular extracts, which are devoid of 26S proteasome, whereas negligible polyubiquitylation pattern was produced using VHL-null S100 extracts (Fig. 3*B*). Furthermore, robust EPOR ubiquitylation was observed in Ba/F3 cells under normoxia, but not under hypoxia (Fig. 3*C*). CRISPR/Cas9 was used to generate UT-7 cells devoid of VHL (Fig. 3*D*). Loss of VHL was associated with decreased level of *in vivo* ubiquitylation of endogenous EPOR (Fig. 3*E*). These results suggest that VHL binds to and promotes the ubiquitylation of EPOR, leading to its increased turnover in an oxygen-dependent manner.

PHD3 Hydroxylates EPOR on Proline 419 and 426—Considering the oxygen-dependent nature of EPOR turnover and binding to VHL, reminiscent of the interaction between HIFα

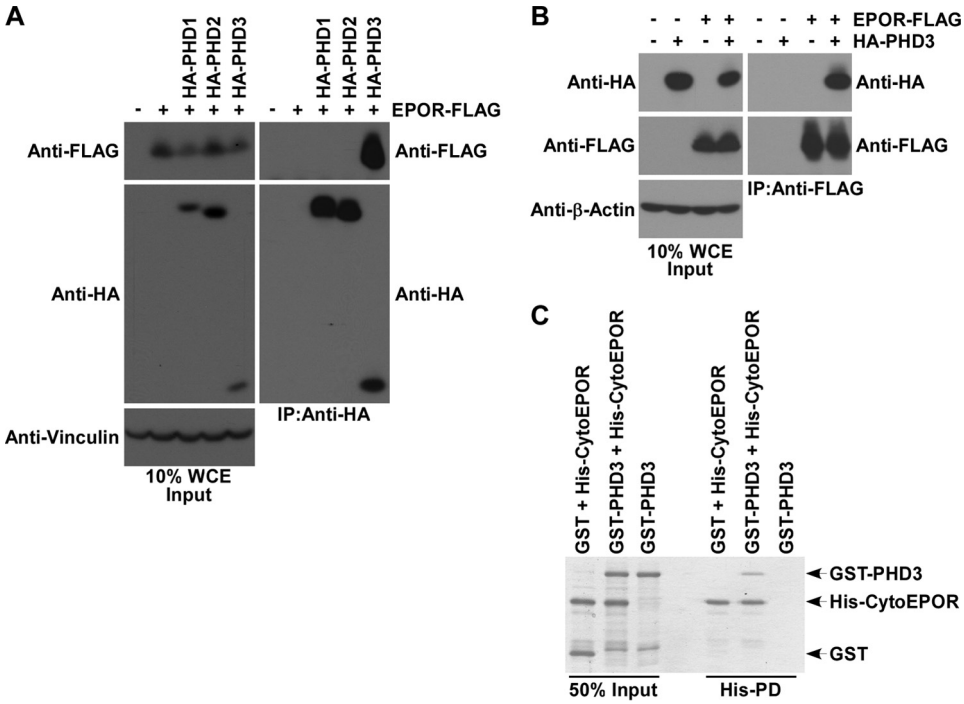

FIGURE 4. **PHD3 binds to EPOR.** *A* and *B*, HEK293 cells were transfected with the indicated plasmids. The cells were treated with 10 μM MG132 for 4 h, lysed, and immunoprecipitated using the indicated antibody. Bound proteins were resolved by SDS-PAGE and detected by immunoblotting with the indicated antibodies. *C*, the indicated recombinant proteins were mixed and a His pulldown was performed using Ni-NTA-agarose. The proteins were visualized by staining with GelCode. *WCE*, whole cell extract; *IP*, immunoprecipitation; *His-PD*, His pulldown. All experiments were performed at least three times.

and VHL, we asked whether PHD enzymes bind EPOR and, if so, whether they promote oxygen-dependent modification of EPOR. Interestingly, EPOR-FLAG preferentially co-precipitated PHD3 and negligibly PHD1 and PHD2 (Fig. 4, *A* and *B*). In addition, recombinant GST-PHD3 bound specifically to purified His-CytoEPOR (Fig. 4*C*). These results suggest that the binding between EPOR and PHD3 is direct. An *in vitro* hydroxylation reaction was then performed using purified GST-PHD3 and His-CytoEPOR followed by mass spectrometry, which identified hydroxylation of Pro^{419} and Pro^{426} (Fig. 5*A*). Furthermore, hydroxylation is a chemical reaction that absolutely requires oxygen; thus, hydroxylation does not occur in the absence of oxygen. Interestingly, Pro^{426} is highly conserved in several organisms examined, and although Pro^{419} appears to be well conserved in the alignment, Pro^{419}, unlike Pro^{426}, is not part of a diprolyl motif (Fig. 5*B*). However, oxygen-dependent prolyl-hydroxylation on endogenous EPOR could not be formally determined via mass spectrometry, at least in part because less than 1% of the total cellular endogenous EPORs are on the cell surface (39) and because of the limitation of the available anti-EPOR antibodies. Notably, prolyhydroxylation of endogenous HIF1α, as well as HIF2α or HIF3α, has not been formally confirmed via mass spectrometry.

EPOR Hydroxylation Is a Prerequisite for VHL Binding—We next asked whether EPOR prolyl hydroxylation is required for binding to VHL. An *in vitro* hydroxylation reaction was first performed on biotinylated 15-amino acid PEP6 peptides spanning Pro^{419} and Pro^{426} in the presence of *in vitro* translated PHD3(WT), catalytically inactive PHD3(H196A), or empty plasmid. PEP6 peptide preincubated with PHD3(WT), but not with PHD3(H196A), bound to *in vitro* translated 3×FLAG-VHL (Fig. 6, *A* and *B*). Biotinylated HIF1α ODD peptide was used to validate that the enzyme was indeed functional, and synthetically hydroxylated ODD peptide (ODD-OH) served as a positive control for binding to VHL (Fig. 6*A*). Similar results were observed using bacterially purified GST-PHD3 in promoting ODD(WT) and PEP6 binding to 3×FLAG-VHL (Fig. 6*C*). We next generated PEP6 peptides with a single synthetic hydroxyl group on Pro^{419}, Pro^{425}, or Pro^{426} and performed an *in vitro* binding assay with HA-VHL. Pro^{419}-OH peptide bound most robustly to HA-VHL, followed by Pro^{426}-OH, whereas Pro^{425}-OH and the unhydroxylated PEP6(WT) showed negligible interaction with HA-VHL (Fig. 6*D*). Notably, Pro^{425} was not identified as a hydroxylation site via MS (Fig. 3*C*). Pro^{419}-OH peptide did not bind to SOCS3, which recognizes phosphorylated EPOR (Fig. 6*E*). These results suggest that Pro^{419} is the major site on CytoEPOR for PHD3-dependent hydroxylation, which is required for binding to VHL.

The bacterially purified GST-VBC complex bound to Pro^{419}-OH, but not to the unhydroxylated Pro^{419} peptide (Fig. 6*F*). Pro^{419}-OH, but not Pro^{419} peptide, co-precipitated VHL and Cul2 in Ba/F3-EPOR cells (Fig. 6*G*). Furthermore, Pro^{419}-OH co-precipitated Cul2 and elongin B only in the presence of VHL (Fig. 6*H*), which suggests that the recruitment of ECV ubiquitin ligase components by Pro^{419}-OH is via binding to VHL.

We showed that, similar to HIFα, EPOR binds to the β domain of VHL (Fig. 2*B*). Consistent with this notion, increased concentration of exogenous ODD-OH attenuated the interaction between HA-VHL and EPOR-FLAG in HEK293 cells (Fig. 6*I*). Unhydroxylatable ODD(P564A) peptide failed to block the interaction between HA-VHL and EPOR-FLAG (Fig. 6*I*). These

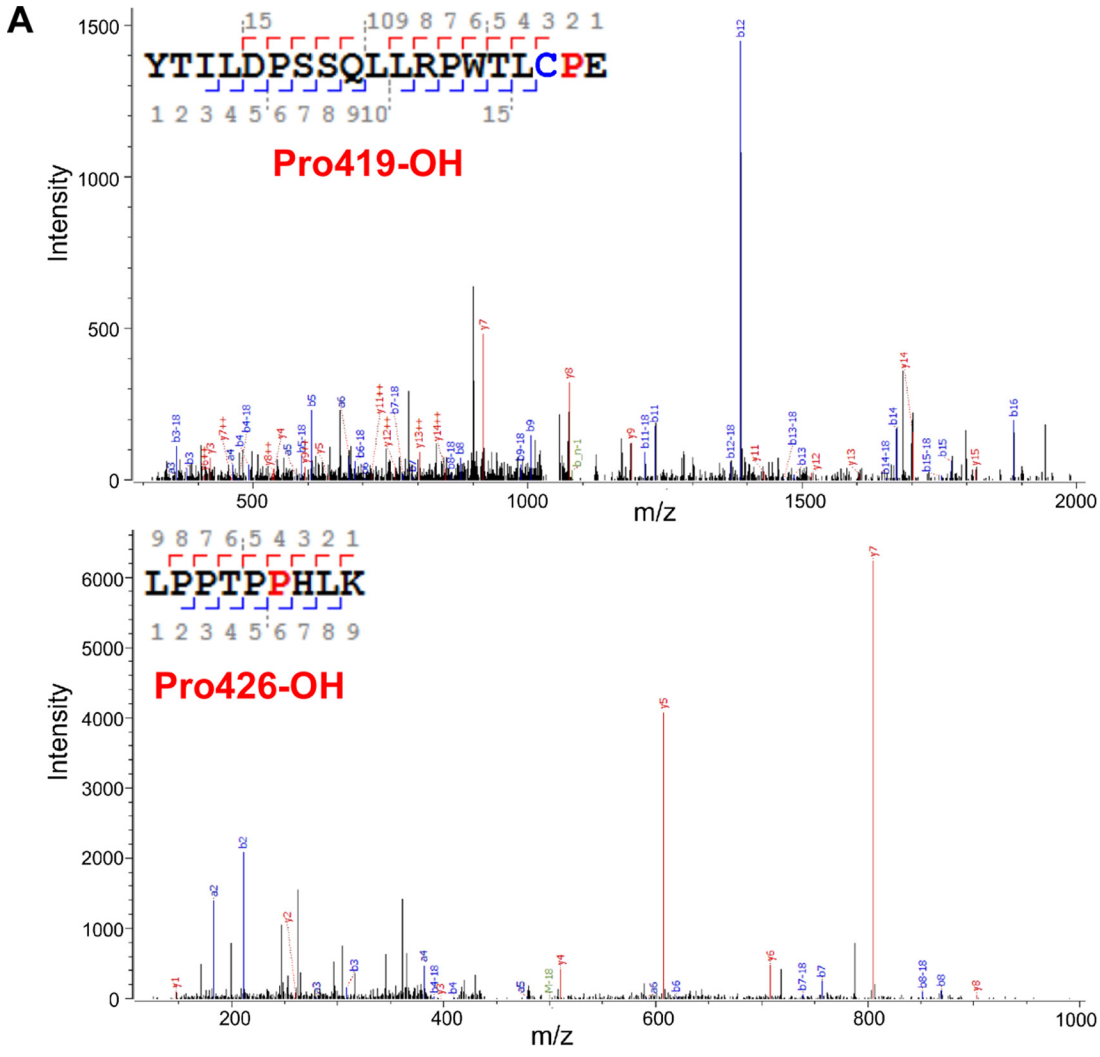

B

H.sapiens	NP_000112.1	LASKPSPEGASAASFEYTILDPSSQLLRPWTLCPELPPTPPHLKYLYLVV 435
P.troglodytes	XP_003953409.1	LASKPSPEGASAASFEYTILDPSSQLLRPWTLCPELPPTPPHLKYLYLVV 447
M.mulatta	XP_001105833.1	LASKPSPEGASAASFEYTILDPSSQLLRPWALSPELPSTPPHLKYLYLVV 435
C.lupus	NP_001041576.1	LSLKPGPEGALGASFEYTILDPSSQLLCPRALPPELPPTPPHIKYLYLMV 435
B.taurus	NP_001192530.1	LALKPGPEGASATSFEYTILDPSSQLLRPRALPPELLPTPPHLKYLYLVV 435
M.musculus	NP_034279.3	LASKPRPEGTSPSSFEYTILDPSSQLLCPRALPPELPPTPPHLKYLYLVV 434
R.norvegicus	NP_058698.2	LASKPRPEGTSPSSFEYTILDPSSKLLCPRALPPELPPTPPHLKYLYLVV 434
D.rerio	NP_001036799.1	LGSLRQSSASGRLSSQSSFEDPN----HPW------PPKGP--GYAYMAV 459

FIGURE 5. **PHD3 hydroxylates EPOR.** *A*, the purified proteins used in Fig. 4*C* were used to perform an *in vitro* hydroxylation reaction. His-huCytoEPOR was digested, and the peptides were analyzed by mass spectrometry. *Red* denotes hydroxylated Pro, whereas *blue* represents alkylated Cys. *B*, an alignment of PEP6 derived from humans was performed against the indicated organisms using NCBI Homologene. * denotes a hydroxylated Pro residue identified by mass spectrometry in human EPOR. *Red* represents PP motifs, whereas *yellow* highlights LCP. Note that for *Danio rerio* the signal peptide length was unknown so it was included in the numbering.

results further support the notion that EPOR and HIFα share an overlapping binding site on VHL. GAL4-HA-PEP6(PPPPPP) (amino acids 412–446 of EPOR) was able to bind to 3×FLAG-VHL (Fig. 6*J*). Notably, mutation of every proline within PEP6 to alanine markedly decreased its interaction to 3×FLAG-VHL (Fig. 6*J*).

We next performed biolayer interferometry analysis to determine the binding kinetics of the interaction between single (Pro^{419} or Pro^{426}) or double (Pro^{419} and Pro^{426}) hydroxylated or unhydroxylated EPOR peptide and bacterially purified ternary complex comprised of VHL, elongin B, and elongin C (VBC) (Table 1 and Fig. 7). The single Pro^{419}-OH peptide had a K_d of 41 nM, and the double Pro^{419}-OH/Pro^{426}-OH peptide had a K_d of 38 nM. However, single Pro^{426}-OH had very weak binding. Notably, ODD-Pro^{564}-OH peptide had a K_d of 31 nM, which is tightly comparable with Pro^{419}-OH. As expected, both unhydroxylated ODD and the unhydroxylated EPOR peptide failed to bind the VBC complex. These results indicate that the hydroxylation of Pro^{419} is critical for promoting the high affinity interaction to VHL and that hydroxylation of Pro^{426} has a minor or negligible influence on the binding between EPOR and VHL.

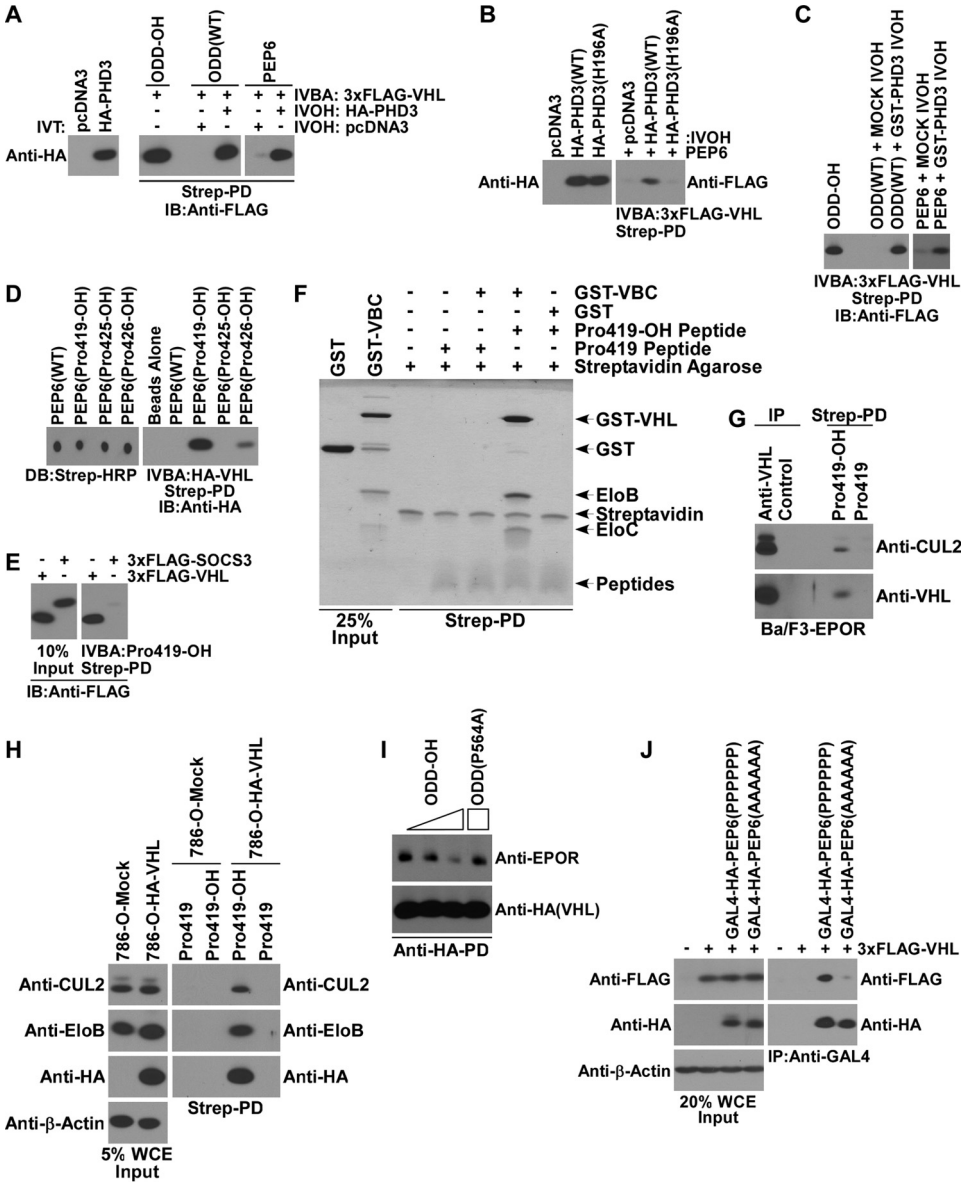

FIGURE 6. **VHL binds prolyl hydroxylated EPOR.** *A* and *B*, an *in vitro* hydroxylation reaction was performed on the indicated biotinylated peptides using *in vitro* translated PHD3 enzyme. Afterward, an *in vitro* binding assay was performed using *in vitro* translated 3×FLAG-VHL. A streptavidin pulldown was performed, and bound VHL was detected by immunoblotting. *C*, an *in vitro* hydroxylation reaction was performed on biotinylated-PEP6 peptide or biotinylated HIF1α(ODD) peptide using purified GST-PHD3 followed by binding to *in vitro* translated 3×FLAG-VHL. *D*, PEP6 that was chemically synthesized to contain hydroxyproline at the indicated residues was attached to streptavidin-agarose. Binding to *in vitro* translated HA-VHL was assessed. Dot blotting was performed to assess the quantity of peptide. *E*, *in vitro* translated 3×FLAG-VHL and 3×FLAG-SOCS3 were incubated with biotinylated Pro^{419}-OH peptide, which was prebound to streptavidin-agarose. Efficiency of binding to Pro^{419}-OH peptide was assessed by anti-FLAG immunoblotting. *F*, the indicated peptides were bound to streptavidin-agarose. GST or GST-VBC was incubated with the peptides, the beads were washed, and proteins were eluted in sample buffer. Protein was resolved by SDS-PAGE and visualized by GelCode staining. *G*, Ba/F3-EPOR cells were lysed. The cell lysate was incubated with Pro^{419} or Pro^{419}-OH peptide that was bound to streptavidin-agarose. In parallel, an anti-VHL or control immunoprecipitation was performed. The beads were washed, and bound proteins were eluted by boiling in sample buffer. The indicated proteins were detected by immunoblotting. *H*, 786-O-Mock and 786-O-HA-VHL cell lysate was incubated with Pro^{419} or Pro^{419}-OH peptide that was prebound to streptavidin-agarose. Interacting proteins were detected through immunoblotting with the indicated antibodies. *I*, HEK293 cells were transfected with HA-VHL and EPOR. The complex was isolated onto beads using HA-agarose and split into four identical tubes that were then incubated with the indicated peptides. Amount of EPOR that remained bound to HA-VHL was detected through immunoblotting. *J*, HEK293 cells were transfected with the indicated plasmids. The cells were treated with 10 μM MG132 for 4 h, lysed, and immunoprecipitated using the indicated antibody. The bound proteins were resolved by SDS-PAGE and detected by immunoblotting with the indicated antibodies. *IB*, immunoblot; *DB*, dot blot; *IP*, immunoprecipitation; *Strep-PD*, streptavidin-agarose pulldown; *IVBA*, *in vitro* binding assay; *IVOH*, *in vitro* hydroxylation. All experiments were performed at least three times.

PHD3 and VHL Negatively Regulate EPOR Signaling—Diminishing oxygen tension was associated with increasing EPOR expression level and downstream signaling in the presence of constant EPO concentration (Fig. 1*C*). We next asked whether the loss of PHD3 or VHL directly influences EPOR expression level and JAK2-STAT5 signaling. ShRNA-mediated knockdown of PHD3 in MEFs increased the expression level of EPOR-FLAG (Fig. 8*A*). Furthermore, UT-7 polyclonal stable cell lines expressing shRNA targeting PHD3, VHL, or nontargeting control (pGIPZ) were maintained in EPO for *in vitro* differentiation analysis (Fig. 8*B*). UT-7 cells are one of a handful of cell lines that are able to initiate hemoglobinization in

TABLE 1
Kinetic parameters of VBC complex binding to substrate peptides

Peptide	VBC Complex		
	K_d	k_a (× 10^5)	k_d (× 10^3)
	nM	$M^{-1}s^{-1}$	s^{-1}
HIF1α-Pro^{564}-OH	31 ± 9	1.3 ± 0.3	3.7 ± 0.1
EPOR-Pro^{419}-OH, Pro^{426}	41 ± 5	2.1 ± 0.2	8.41 ± 0.03
EPOR-Pro^{419}-OH, Pro^{426}-OH	38 ± 8	2.6 ± 0.3	10 ± 3
EPOR-Pro^{419}, Pro^{426}-OH	Low binding (> μM)		
EPOR-Pro^{419}, Pro^{426}	No binding		

response to EPO stimulus. Differentiation of these UT-7 cells in the presence of EPO, but not GM-CSF, was also visibly noticeable with increased redness (Fig. 8*B*) (44). Notably, spectrophotometric quantification revealed a statistically significant increase in hemoglobinization in UT-7-shPHD3 and UT-7-shVHL cell lines as compared with control UT-7-pGIPZ cells (Fig. 8*B*). CRISPR/Cas9 system (36) was used to knock out the endogenous *PHD3* or *VHL* in UT-7 cells (Figs. 8*C* and 3*D*, respectively). The cell surface of knock-out UT-7 cells and parental UT-7 cells was biotinylated. Subsequent streptavidin pulldown assay showed that VHL-null and PHD3-null cells had higher amounts of cell surface EPOR (Fig. 9*A*). In comparison with wild-type UT-7 cells, UT-7(*PHD3*$^{-/-}$) and UT-7 (*VHL*$^{-/-}$) cells had greater amplitude in signaling as measured by increased levels of phosphorylated EPOR, JAK2, and STAT5 upon EPO stimulation following cytokine starvation (Figs. 8*D* and 9*B*, respectively). Reconstitution of UT-7(*VHL*$^{-/-}$) cells with HA-VHL(WT) restored the reduced EPOR signaling compared with GFP expressing control cells (Fig. 9*C*). These results support the notion that PHD3 and VHL negatively regulate EPOR signaling and potentially influence EPOR-dependent physiologic response.

VHL disease has several phenotypic manifestations. Using several known type 2-associated mutants (13, 14) (type 2A is associated with the development of PHEO and HAB with a low risk of RCC, type 2B is associated with PHEO and HAB with a high risk of RCC, and type 2C is associated exclusively with PHEO), we asked whether any of the VHL mutants exhibited a defect in binding to EPOR Pro^{419}-OH peptide as well as to HIF1αODD-OH. In comparison with *in vitro* translated VHL(WT), type 2A and type 2B *in vitro* translated VHL mutants displayed reduced binding to ODD-OH as previously described (13, 14), but these deficiencies were more pronounced for Pro^{419}-OH (Fig. 9*D*). As expected, VHL(WT) bound to the hydroxylated Pro^{419}-OH or ODD-OH peptides but not to the unhydroxylated peptides (Fig. 9*D*). Unlike type 2A/B, type 2C mutants have been generally reported to retain the binding to and regulation of HIF1α (13, 14). Consistent with these findings, three of five type 2C mutants tested, namely VHL(R64P), VHL(V84L), and VHL(L188V), showed relatively robust binding to ODD-OH (Fig. 9*D*). Notably, all type 2C mutants tested showed a marked defect in binding to Pro^{419}-OH (Fig. 9*D*). Consistent with these observations, both ODD-OH and Pro^{419}-OH peptides bound robustly to ectopically expressed HA-VHL(WT), whereas Pro^{419}-OH peptide, but not ODD-OH, showed markedly reduced binding to ectopically expressed HA-VHL(R64P) in HEK293 cells (Fig. 9*E*). Moreover, HA-VHL(R64P) showed attenuated binding to full-length EPOR-FLAG compared with HA-VHL(WT) (Fig. 9*F*).

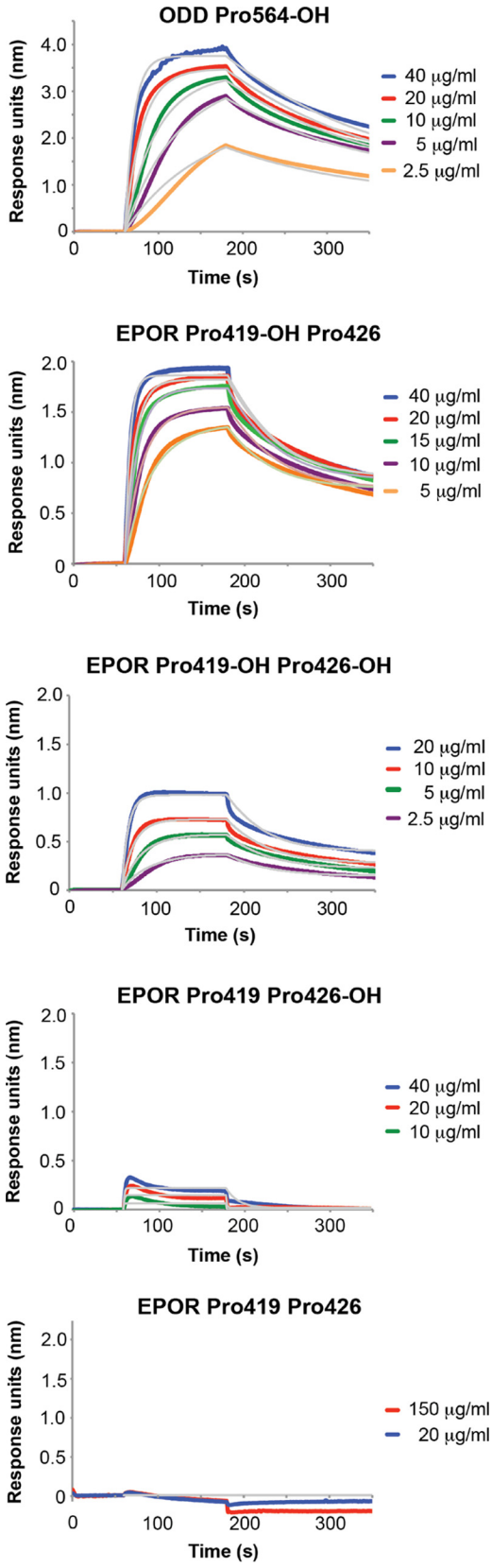

FIGURE 7. **Biolayer interferometry kinetic analysis of VBC binding to EPOR and ODD peptides.** Biotin-labeled peptides were coupled to streptavidin-coated biosensors and monitored for binding to purified 1:1:1 VBC complex at the indicated concentrations. The data were analyzed based on a 1:1 binding model using the BLItz Pro software with the *fitted curves* shown as *gray lines* based on a representative experiment. The kinetics experiment was performed twice.

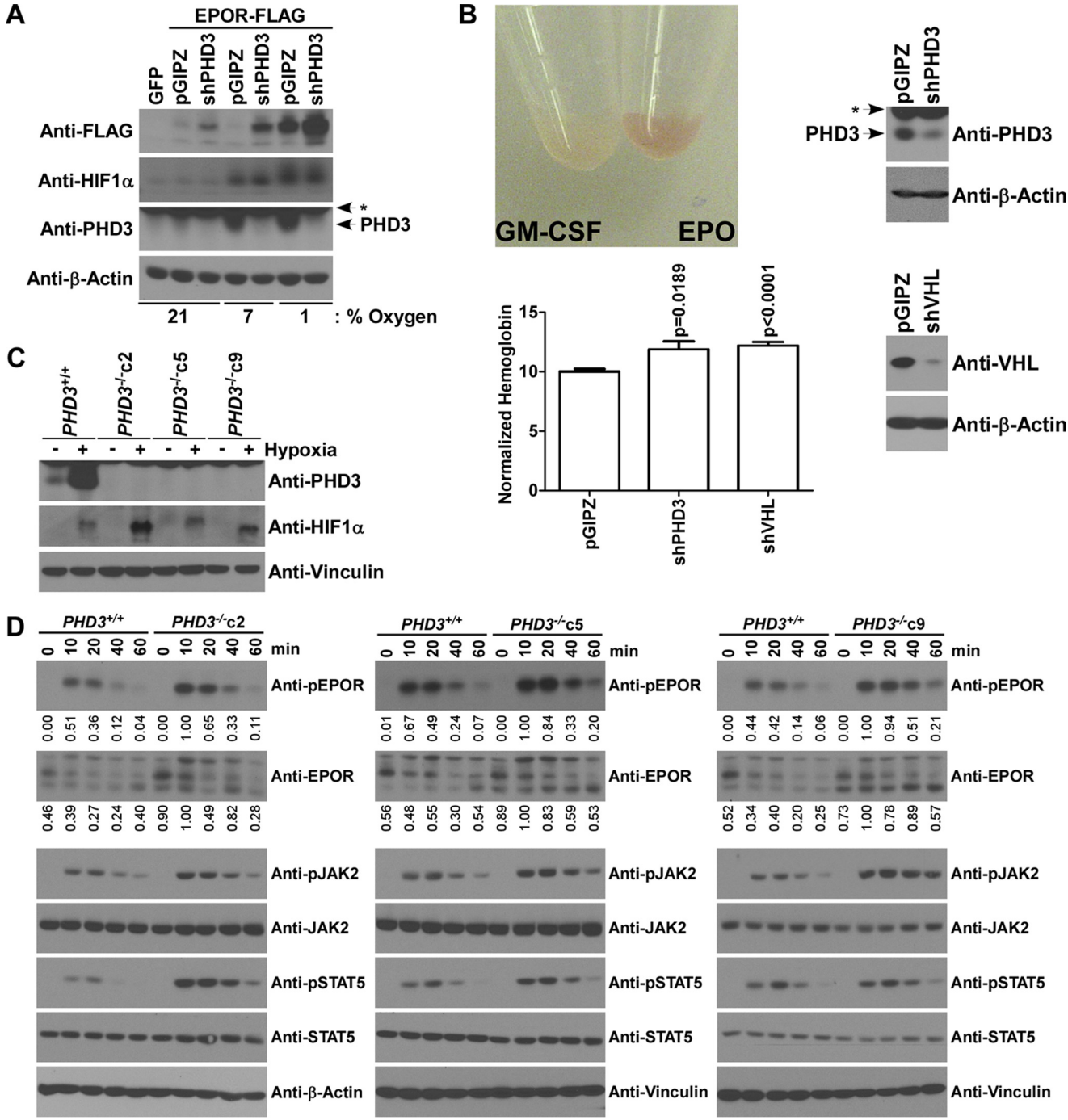

FIGURE 8. **EPOR signaling can be modulated by PHD3.** *A*, MEF cells expressing EPOR-FLAG were infected using pGIPZ control or shPHD3 lentivirus. The cells were maintained at the indicated oxygen tension overnight. The cells were lysed and resolved by SDS-PAGE, and immunoblotting was performed using the indicated antibodies. *B*, *in vitro* differentiation assay was performed three independent times on UT-7 cells stably expressing the indicated shRNA constructs. A Student's *t* test was used to assess the statistical significance. *C*, parental UT-7 cells or the indicated clones were assessed for CRISPR-Cas9-mediated gene editing. The cells were maintained in hypoxia overnight where indicated. The cells were lysed, and the indicated proteins were detected by immunoblotting. *D*, UT-7 parental cells or the indicated *PHD3*$^{-/-}$ clones were cytokine-starved overnight. The cells were treated with 1 unit/ml EPO for the indicated amount of time. The proteins were visualized by immunoblotting with the indicated antibodies. Densitometry values were normalized to loading control. * denotes a nonspecific band.

Discussion

Red blood cell production is a key physiologic response to hypoxia that allows the body to increase its oxygen carrying capacity. Erythropoiesis is strictly dependent upon the cytokine EPO with the output signaling being governed by erythroid cell intrinsic proteins (23). EPO production is regulated through an oxygen-sensitive extrinsic PHD2-HIF2α-VHL axis (17–21, 29). Here we identify an additional oxygen-sensitive pathway comprised of an intrinsic PHD3-EPOR-VHL axis that can modulate the duration and amplitude of EPO-based signaling by regulating the cell surface expression level of EPOR.

We show here that EPOR is hydroxylated on prolines at positions 419 and 426 within the cytoplasmic region by PHD3. However, hydroxylation of Pro^{419} appears to be a key event that

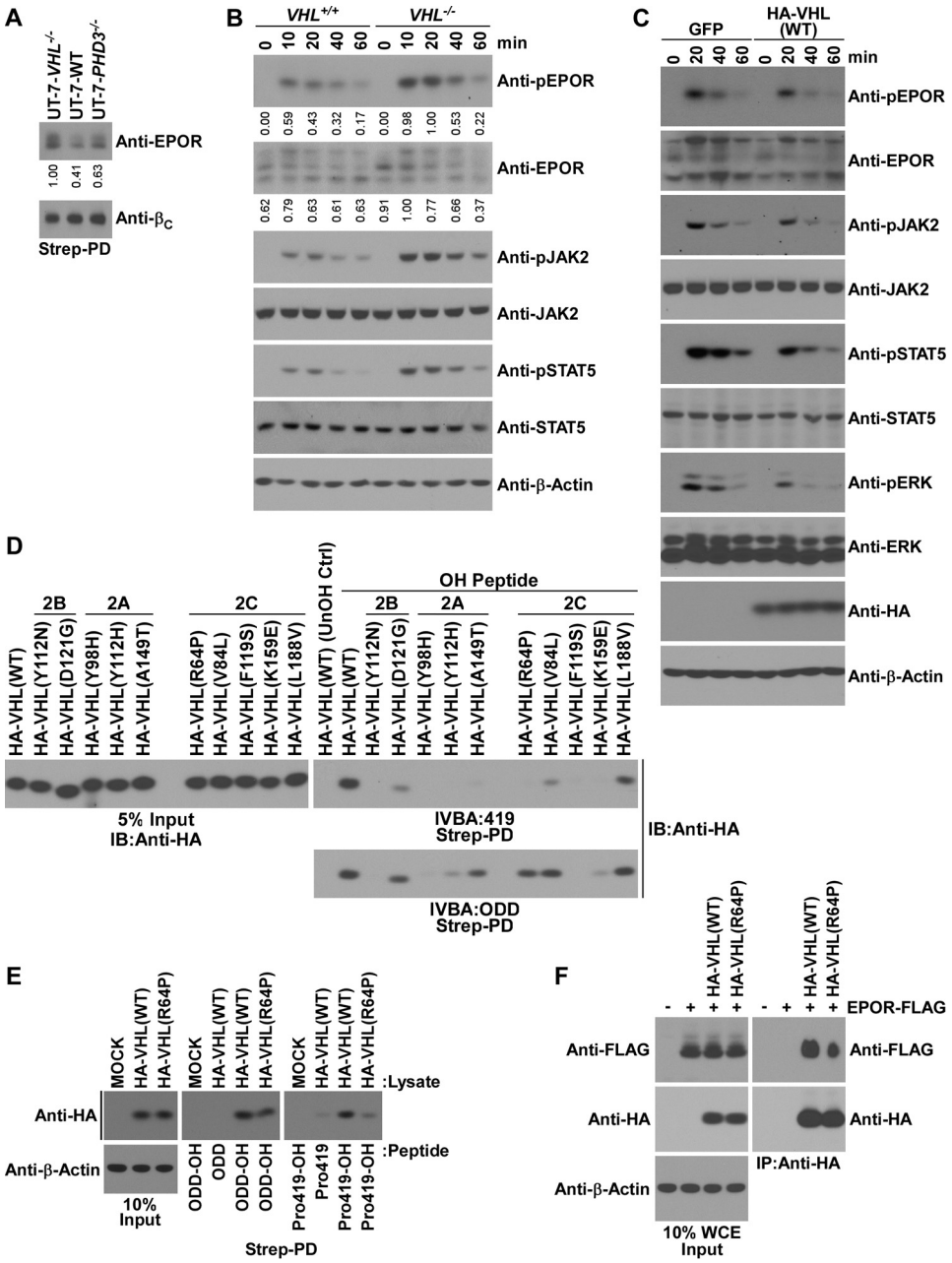

FIGURE 9. **EPOR signaling can be modulated by VHL.** *A*, an equivalent number of cells from the indicated cell lines was cell surface-biotinylated. A streptavidin pulldown was performed to enrich the biotinylated proteins, which were eluted and resolved by SDS-PAGE. The indicated proteins were detected by immunoblotting. EPOR signals were measured by densitometry and normalized to βc. *B*, UT-7 parental cells or UT-7 *VHL* knock-out cells were cytokine-starved overnight. The cells were treated with 1 unit/ml EPO for the indicated amount of time. The proteins were visualized by immunoblotting with the indicated antibodies. The experiments were performed in triplicate. Densitometry values were normalized to β-actin. *C*, VHL-null UT-7 cells were infected with lentivirus containing GFP or HA-VHL(WT). The cells were cytokine-starved overnight. The cells were treated with 1 unit/ml EPO for the indicated amount of time. Proteins were visualized by immunoblotting with the indicated antibodies. *D*, the indicated VHL constructs were *in vitro* translated using rabbit reticulocyte lysate that was incubated with Pro^{419}-OH or ODD-OH peptides (or unhydroxylated control peptides) prebound to streptavidin-agarose. VHL binding was assessed by anti-HA immunoblotting. *E*, the indicated peptides were attached onto streptavidin-agarose. The beads were incubated with the indicated HEK293 transfected lysates. The beads were washed, and interacting proteins were resolved by SDS-PAGE and detected by immunoblotting. *F*, HEK293 cells were transfected with the indicated plasmids. The cells were lysed, and anti-HA immunoprecipitation was performed. The proteins were resolved by SDS-PAGE and detected by immunoblotting using the indicated antibodies. *WCE*, whole cell extract; *IP*, immunoprecipitate; *IVBA*, *in vitro* binding assay; *Strep-PD*, streptavidin-agarose pulldown; *Ctrl*, control.

marks EPOR for VHL recognition and subsequent ECV-mediated ubiquitylation under normoxia. Hypoxia or the molecular inhibition of PHD3 or VHL attenuates EPOR turnover, resulting in an increased JAK2-STAT5 signaling in the presence of EPO. Notably, Pro^{419} is within a region of EPOR that contains numerous negative regulatory signals. For example, adjacent are Tyr^{430} and Tyr^{432} (Tyr^{429} and Tyr^{431} in mice), which upon EPO engagement and JAK2 phosphorylation promote EPOR endocytosis (45). EPO stimulation also promotes binding to and negative regulation by β-TrCP in a Ser^{438}-dependent manner (40). EPOR truncations are commonly found in patients with primary familial and congenital polycythemia. Interest-

ingly, these mutations have been shown to lead to the accumulation of truncated EPOR at the plasma membrane, which is thought to underlie increased downstream signaling (24, 25). Perhaps most notably, many of the disease-associated truncations eliminate Pro^{419} (and Pro^{426}), which is predicted to cause a failure in the negative regulation of EPOR via VHL and a consequential prolongation of cell surface EPOR expression. Future experiments would be needed to address the factors and processes controlling hydroxylation of endogenous EPOR and the specific role of Pro^{419}.

At present it is unclear why a loss of both PHD1 and PHD3 is required to produce a hematologic phenotype in mice (30). Recently, PHD1 was shown to hydroxylate FOXO3a to promote its degradation through a mechanism that does not seemingly involve VHL (46). FOXO3a has been reported to promote the expression of antioxidant genes that through their regulation of ROS determine the lifespan of a circulating red blood cell (47). We show here that a loss of PHD3 leads to exaggerated EPO-mediated signaling via EPOR up-regulation. Thus, the aforementioned effects when combined upon the loss of both PHD1 and PHD3 might have contributed to the development of polycythemia in these double knock-out mice despite exhibiting reduced serum EPO level.

It is also unclear at present what determines the genotype-phenotype correlation observed in VHL disease. We show here that ODD-OH and Pro^{419}-OH peptides share an overlapping binding region on VHL within the β domain. It is perhaps not surprising then that type 2A and 2B disease-associated VHL mutants, which are known to have a defect in binding to HIFα, show a similar defect in binding to Pro^{419}-OH. Type 2C mutations, which cause PHEO without other manifestation of VHL disease, have been generally regarded to retain the capacity to negatively regulate HIFα (13, 14). In contrast, type 2C mutants showed a marked defect in binding to Pro^{419}-OH. For example, R64P, V84L, and L188V mutants, which have comparable binding to ODD-OH as wild-type VHL, showed negligible to modest binding to Pro^{419}-OH. These results suggest the possibility and significance of a loss of EPOR regulation via VHL in the pathogenesis of PHEO.

Several studies have suggested a potential involvement of PHD3 in PHEO. At a cellular level, PHEO arises from the increased survival or decreased apoptosis of sympathetic neuronal progenitor cells. Kaelin and co-workers (35) have shown that the overexpression of catalytically active PHD3 in PC12 PHEO cells leads to apoptosis. The target of PHD3 in PHEO is unknown. Although it is formally unknown whether EPOR is a relevant target of PHD3 in PHEO, EPO treatment of PC12 and neuroblastoma SH-SY5Y cells was shown to be protective against apoptosis (48, 49), which strongly suggests EPOR expression in these cell types. Furthermore, $Phd3^{-/-}$ mice have increased numbers of sympathetic neurons (50), and PHD3 (R8S) mutation was identified in a patient with PHEO (51). Whether these phenomena are attributable at least in part to elevated EPOR dependent pro-survival signaling remains an outstanding question.

Furthermore, although individuals with $VHL^{R200W/WT}$ genotype do not display features of polycythemia, two polycythemia patients with $VHL^{R200W/L188V}$ genotype have been reported; one of them had a normal serum EPO level (52, 53). These findings, although limited, suggest that an impaired VHL-mediated EPOR degradation could be a contributing factor in the development of polycythemia. Consistent with this notion, PHD3 was identified in an shRNA screen on patient-derived hematopoietic progenitor cells that when lost would promote longer stem cell maintenance or increased growth (54).

HAB of the retina and central nervous system (cerebellum, brainstem and spinal cord) is a cardinal feature of VHL disease. A hemangioblast is a cell that is capable of differentiating into endothelial and hematopoietic cells. Consistent with this notion, islands of blood cells are often found within HAB (55–57). In addition, studies have suggested that HAB potentially express EPOR (56). These observations suggest that a failure in the proper negative regulation of EPOR in addition to the predicted up-regulation of EPO production upon the loss or mutation of VHL plays a role in the development of HAB.

These results, taken together, identify EPOR as a substrate of PHD3, which upon oxygen-dependent prolyl hydroxylation is targeted for VHL-mediated ubiquitylation and subsequent degradation. It remains an outstanding question whether the oxygen-dependent negative regulation of EPOR via VHL plays a critical role in normal erythropoiesis, as well as in the pathogenesis of VHL disease upon the loss of this newly defined function of VHL.

Author Contributions—P. H. designed, performed and interpreted the experiments, conceptualized the project, and wrote the manuscript. T. S. designed, performed, and interpreted the MS data. G. B. designed and performed the BLItz experiments and purified the VBC complex. S. B. designed and performed *in vitro* experiments and microscopy. B. P. P. designed and performed *in vitro* experiments. J. E. L. designed and interpreted the BLItz experiments. B. R. designed and interpreted the MS experiments. M. O. conceptualized the project, interpreted the data, and wrote the manuscript.

Acknowledgments—We thank Dr. Arianna Rath and Dr. Charles Deber for assistance in designing EPOR peptides.

References

1. Richard, S., Gardie, B., Couvé, S., and Gad, S. (2013) Von Hippel-Lindau: how a rare disease illuminates cancer biology. *Semin. Cancer Biol.* **23,** 26–37
2. Kim, W. Y., and Kaelin, W. G. (2004) Role of VHL gene mutation in human cancer. *J. Clin, Oncol.* **22,** 4991–5004
3. Ohh, M., Park, C. W., Ivan, M., Hoffman, M. A., Kim, T. Y., Huang, L. E., Pavletich, N., Chau, V., and Kaelin, W. G. (2000) Ubiquitination of hypoxia-inducible factor requires direct binding to the β-domain of the von Hippel-Lindau protein. *Nat. Cell Biol.* **2,** 423–427
4. Ivan, M., Kondo, K., Yang, H., Kim, W., Valiando, J., Ohh, M., Salic, A., Asara, J. M., Lane, W. S., and Kaelin, W. G., Jr. (2001) HIFα targeted for VHL-mediated destruction by proline hydroxylation: implications for O2 sensing. *Science* **292,** 464–468
5. Jaakkola, P., Mole, D. R., Tian, Y. M., Wilson, M. I., Gielbert, J., Gaskell, S. J., von Kriegsheim, A., Hebestreit, H. F., Mukherji, M., Schofield, C. J., Maxwell, P. H., Pugh, C. W., and Ratcliffe, P. J. (2001) Targeting of HIF-α to the von Hippel-Lindau ubiquitylation complex by O_2-regulated prolyl hydroxylation. *Science* **292,** 468–472
6. Epstein, A. C., Gleadle, J. M., McNeill, L. A., Hewitson, K. S., O'Rourke, J., Mole, D. R., Mukherji, M., Metzen, E., Wilson, M. I., Dhanda, A., Tian, Y. M., Masson, N., Hamilton, D. L., Jaakkola, P., Barstead, R., Hodgkin, J.,

Maxwell, P. H., Pugh, C. W., Schofield, C. J., and Ratcliffe, P. J. (2001) *C. elegans* EGL-9 and mammalian homologs define a family of dioxygenases that regulate HIF by prolyl hydroxylation. *Cell* **107,** 43–54
7. Bruick, R. K., and McKnight, S. L. (2001) A conserved family of prolyl-4-hydroxylases that modify HIF. *Science* **294,** 1337–1340
8. Semenza, G. L. (2011) Oxygen sensing, homeostasis, and disease. *N. Engl. J. Med.* **365,** 537–547
9. Kuznetsova, A. V., Meller, J., Schnell, P. O., Nash, J. A., Ignacak, M. L., Sanchez, Y., Conaway, J. W., Conaway, R. C., and Czyzyk-Krzeska, M. F. (2003) von Hippel-Lindau protein binds hyperphosphorylated large subunit of RNA polymerase II through a proline hydroxylation motif and targets it for ubiquitination. *Proc. Natl. Acad. Sci. U.S.A.* **100,** 2706–2711
10. Okuda, H., Saitoh, K., Hirai, S., Iwai, K., Takaki, Y., Baba, M., Minato, N., Ohno, S., and Shuin, T. (2001) The von Hippel-Lindau tumor suppressor protein mediates ubiquitination of activated atypical protein kinase C. *J. Biol. Chem.* **276,** 43611–43617
11. Anderson, K., Nordquist, K. A., Gao, X., Hicks, K. C., Zhai, B., Gygi, S. P., and Patel, T. B. (2011) Regulation of cellular levels of Sprouty2 protein by prolyl hydroxylase domain and von Hippel-Lindau proteins. *J. Biol. Chem.* **286,** 42027–42036
12. Xie, L., Xiao, K., Whalen, E. J., Forrester, M. T., Freeman, R. S., Fong, G., Gygi, S. P., Lefkowitz, R. J., and Stamler, J. S. (2009) Oxygen-regulated β_2-adrenergic receptor hydroxylation by EGLN3 and ubiquitylation by pVHL. *Sci. Signal.* **2,** ra33
13. Clifford, S. C., Cockman, M. E., Smallwood, A. C., Mole, D. R., Woodward, E. R., Maxwell, P. H., Ratcliffe, P. J., and Maher, E. R. (2001) Contrasting effects on HIF-1α regulation by disease-causing pVHL mutations correlate with patterns of tumourigenesis in von Hippel-Lindau disease. *Hum. Mol. Genet.* **10,** 1029–1038
14. Hoffman, M. A., Ohh, M., Yang, H., Klco, J. M., Ivan, M., and Kaelin, W. G., Jr. (2001) von Hippel-Lindau protein mutants linked to type 2C VHL disease preserve the ability to downregulate HIF. *Hum. Mol. Genet.* **10,** 1019–1027
15. Ohh, M., Yauch, R. L., Lonergan, K. M., Whaley, J. M., Stemmer-Rachamimov, A. O., Louis, D. N., Gavin, B. J., Kley, N., Kaelin, W. G., Jr., and Iliopoulos, O. (1998) The von Hippel-Lindau tumor suppressor protein is required for proper assembly of an extracellular fibronectin matrix. *Mol. Cell* **1,** 959–968
16. Erslev, A. (1953) Humoral regulation of red cell production. *Blood* **8,** 349–357
17. Kapitsinou, P. P., Liu, Q., Unger, T. L., Rha, J., Davidoff, O., Keith, B., Epstein, J. A., Moores, S. L., Erickson-Miller, C. L., and Haase, V. H. (2010) Hepatic HIF-2 regulates erythropoietic responses to hypoxia in renal anemia. *Blood* **116,** 3039–3048
18. Scortegagna, M., Ding, K., Zhang, Q., Oktay, Y., Bennett, M. J., Bennett, M., Shelton, J. M., Richardson, J. A., Moe, O., and Garcia, J. A. (2005) HIF-2α regulates murine hematopoietic development in an erythropoietin-dependent manner. *Blood* **105,** 3133–3140
19. Rankin, E. B., Biju, M. P., Liu, Q., Unger, T. L., Rha, J., Johnson, R. S., Simon, M. C., Keith, B., and Haase, V. H. (2007) Hypoxia-inducible factor-2 (HIF-2) regulates hepatic erythropoietin *in vivo*. *J. Clin. Invest.* **117,** 1068–1077
20. Gruber, M., Hu, C. J., Johnson, R. S., Brown, E. J., Keith, B., and Simon, M. C. (2007) Acute postnatal ablation of Hif-2α results in anemia. *Proc. Natl. Acad. Sci. U.S.A.* **104,** 2301–2306
21. Kim, W. Y., Safran, M., Buckley, M. R., Ebert, B. L., Glickman, J., Bosenberg, M., Regan, M., and Kaelin, W. G., Jr. (2006) Failure to prolyl hydroxylate hypoxia-inducible factor α phenocopies VHL inactivation *in vivo*. *EMBO J.* **25,** 4650–4662
22. Witthuhn, B. A., Quelle, F. W., Silvennoinen, O., Yi, T., Tang, B., Miura, O., and Ihle, J. N. (1993) JAK2 associates with the erythropoietin receptor and is tyrosine phosphorylated and activated following stimulation with erythropoietin. *Cell* **74,** 227–236
23. Wu, H., Liu, X., Jaenisch, R., and Lodish, H. F. (1995) Generation of committed erythroid BFU-E and CFU-E progenitors does not require erythropoietin or the erythropoietin receptor. *Cell* **83,** 59–67
24. Motohashi, T., Nakamura, Y., Osawa, M., Hiroyama, T., Iwama, A., Shibuya, A., and Nakauchi, H. (2001) Increased cell surface expression of C-terminal truncated erythropoietin receptors in polycythemia. *Eur. J. Haematol.* **67,** 88–93
25. Perrotta, S., Cucciolla, V., Ferraro, M., Ronzoni, L., Tramontano, A., Rossi, F., Scudieri, A. C., Borriello, A., Roberti, D., Nobili, B., Cappellini, M. D., Oliva, A., Amendola, G., Migliaccio, A. R., Mancuso, P., Martin-Padura, I., Bertolini, F., Yoon, D., Prchal, J. T., and Della Ragione, F. (2010) EPO receptor gain-of-function causes hereditary polycythemia, alters CD34 cell differentiation and increases circulating endothelial precursors. *PLoS One* **5,** e12015
26. Delhommeau, F., Pisani, D. F., James, C., Casadevall, N., Constantinescu, S., and Vainchenker, W. (2006) Oncogenic mechanisms in myeloproliferative disorders. *Cell. Mol. Life Sci.* **63,** 2939–2953
27. Lee, F. S., and Percy, M. J. (2011) The HIF pathway and erythrocytosis. *Annu. Rev. Pathol.* **6,** 165–192
28. Furlow, P. W., Percy, M. J., Sutherland, S., Bierl, C., McMullin, M. F., Master, S. R., Lappin, T. R., and Lee, F. S. (2009) Erythrocytosis-associated HIF-2α mutations demonstrate a critical role for residues C-terminal to the hydroxylacceptor proline. *J. Biol. Chem.* **284,** 9050–9058
29. Arsenault, P. R., Pei, F., Lee, R., Kerestes, H., Percy, M. J., Keith, B., Simon, M. C., Lappin, T. R., Khurana, T. S., and Lee, F. S. (2013) A knock-in mouse model of human PHD2 gene-associated erythrocytosis establishes a haploinsufficiency mechanism. *J. Biol. Chem.* **288,** 33571–33584
30. Takeda, K., Aguila, H. L., Parikh, N. S., Li, X., Lamothe, K., Duan, L. J., Takeda, H., Lee, F. S., and Fong, G. H. (2008) Regulation of adult erythropoiesis by prolyl hydroxylase domain proteins. *Blood* **111,** 3229–3235
31. Minamishima, Y. A., Moslehi, J., Bardeesy, N., Cullen, D., Bronson, R. T., and Kaelin, W. G., Jr. (2008) Somatic inactivation of the PHD2 prolyl hydroxylase causes polycythemia and congestive heart failure. *Blood* **111,** 3236–3244
32. Akahane, K., Tojo, A., Fukamachi, H., Kitamura, T., Saito, T., Urabe, A., and Takaku, F. (1989) Binding of iodinated erythropoietin to rat bone marrow cells under normal and anemic conditions. *Exp. Hematol.* **17,** 177–182
33. Russell, R. C., Sufan, R. I., Zhou, B., Heir, P., Bunda, S., Sybingco, S. S., Greer, S. N., Roche, O., Heathcote, S. A., Chow, V. W., Boba, L. M., Richmond, T. D., Hickey, M. M., Barber, D. L., Cheresh, D. A., Simon, M. C., Irwin, M. S., Kim, W. Y., and Ohh, M. (2011) Loss of JAK2 regulation via a heterodimeric VHL-SOCS1 E3 ubiquitin ligase underlies *Chuvash polycythemia*. *Nat. Med.* **17,** 845–853
34. Campeau, E., Ruhl, V. E., Rodier, F., Smith, C. L., Rahmberg, B. L., Fuss, J. O., Campisi, J., Yaswen, P., Cooper, P. K., and Kaufman, P. D. (2009) A versatile viral system for expression and depletion of proteins in mammalian cells. *PLoS One* **4,** e6529
35. Lee, S., Nakamura, E., Yang, H., Wei, W., Linggi, M. S., Sajan, M. P., Farese, R. V., Freeman, R. S., Carter, B. D., Kaelin, W. G., Jr., and Schlisio, S. (2005) Neuronal apoptosis linked to EglN3 prolyl hydroxylase and familial pheochromocytoma genes: developmental culling and cancer. *Cancer Cell* **8,** 155–167
36. Shalem, O., Sanjana, N. E., Hartenian, E., Shi, X., Scott, D. A., Mikkelsen, T. S., Heckl, D., Ebert, B. L., Root, D. E., Doench, J. G., and Zhang, F. (2014) Genome-scale CRISPR-Cas9 knockout screening in human cells. *Science* **343,** 84–87
37. Ivan, M., Haberberger, T., Gervasi, D. C., Michelson, K. S., Günzler, V., Kondo, K., Yang, H., Sorokina, I., Conaway, R. C., Conaway, J. W., and Kaelin, W. G., Jr. (2002) Biochemical purification and pharmacological inhibition of a mammalian prolyl hydroxylase acting on hypoxia-inducible factor. *Proc. Natl. Acad. Sci. U.S.A.* **99,** 13459–13464
38. Gopalakrishnan, T. V., and Anderson, W. F. (1979) Mouse erythroleukemia cells. *Methods Enzymol.* **58,** 506–511
39. Supino-Rosin, L., Yoshimura, A., Altaratz, H., and Neumann, D. (1999) A cytosolic domain of the erythropoietin receptor contributes to endoplasmic reticulum-associated degradation. *Eur. J. Biochem.* **263,** 410–419
40. Meyer, L., Deau, B., Forejtníková, H., Duménil, D., Margottin-Goguet, F., Lacombe, C., Mayeux, P., and Verdier, F. (2007) β-Trcp mediates ubiquitination and degradation of the erythropoietin receptor and controls cell proliferation. *Blood* **109,** 5215–5222
41. Hörtner, M., Nielsch, U., Mayr, L. M., Heinrich, P. C., and Haan, S. (2002) A new high affinity binding site for suppressor of cytokine signaling-3 on

the erythropoietin receptor. *Eur. J. Biochem.* **269,** 2516–2526
42. Sasaki, A., Yasukawa, H., Shouda, T., Kitamura, T., Dikic, I., and Yoshimura, A. (2000) CIS3/SOCS-3 suppresses erythropoietin (EPO) signaling by binding the EPO receptor and JAK2. *J. Biol. Chem.* **275,** 29338–29347
43. Huang, L. J., Constantinescu, S. N., and Lodish, H. F. (2001) The N-terminal domain of Janus kinase 2 is required for Golgi processing and cell surface expression of erythropoietin receptor. *Mol. Cell* **8,** 1327–1338
44. Komatsu, N., Kirito, K., Shimizu, R., Kunitama, M., Yamada, M., Uchida, M., Takatoku, M., Eguchi, M., and Miura, Y. (1997) *In vitro* development of erythroid and megakaryocytic cells from a UT-7 subline, UT-7/GM. *Blood* **89,** 4021–4033
45. Sulahian, R., Cleaver, O., and Huang, L. J. (2009) Ligand-induced EpoR internalization is mediated by JAK2 and p85 and is impaired by mutations responsible for primary familial and congenital polycythemia. *Blood* **113,** 5287–5297
46. Zheng, X., Zhai, B., Koivunen, P., Shin, S. J., Lu, G., Liu, J., Geisen, C., Chakraborty, A. A., Moslehi, J. J., Smalley, D. M., Wei, X., Chen, X., Chen, Z., Beres, J. M., Zhang, J., Tsao, J. L., Brenner, M. C., Zhang, Y., Fan, C., DePinho, R. A., Paik, J., Gygi, S. P., Kaelin, W. G., Jr., and Zhang, Q. (2014) Prolyl hydroxylation by EglN2 destabilizes FOXO3a by blocking its interaction with the USP9x deubiquitinase. *Genes Dev.* **28,** 1429–1444
47. Marinkovic, D., Zhang, X., Yalcin, S., Luciano, J. P., Brugnara, C., Huber, T., and Ghaffari, S. (2007) Foxo3 is required for the regulation of oxidative stress in erythropoiesis. *J. Clin. Invest.* **117,** 2133–2144
48. Um, M., Gross, A. W., and Lodish, H. F. (2007) A "classical" homodimeric erythropoietin receptor is essential for the antiapoptotic effects of erythropoietin on differentiated neuroblastoma SH-SY5Y and pheochromocytoma PC-12 cells. *Cell. Signal.* **19,** 634–645
49. Um, M., and Lodish, H. F. (2006) Antiapoptotic effects of erythropoietin in differentiated neuroblastoma SH-SY5Y cells require activation of both the STAT5 and AKT signaling pathways. *J. Biol. Chem.* **281,** 5648–5656
50. Bishop, T., Gallagher, D., Pascual, A., Lygate, C. A., de Bono, J. P., Nicholls, L. G., Ortega-Saenz, P., Oster, H., Wijeyekoon, B., Sutherland, A. I., Grosfeld, A., Aragones, J., Schneider, M., van Geyte, K., Teixeira, D., Diez-Juan, A., Lopez-Barneo, J., Channon, K. M., Maxwell, P. H., Pugh, C. W., Davies, A. M., Carmeliet, P., and Ratcliffe, P. J. (2008) Abnormal sympathoadrenal development and systemic hypotension in PHD3$^{-/-}$ mice. *Mol. Cell. Biol.* **28,** 3386–3400
51. Astuti, D., Ricketts, C. J., Chowdhury, R., McDonough, M. A., Gentle, D., Kirby, G., Schlisio, S., Kenchappa, R. S., Carter, B. D., Kaelin, W. G., Jr., Ratcliffe, P. J., Schofield, C. J., Latif, F., and Maher, E. R. (2011) Mutation analysis of HIF prolyl hydroxylases (PHD/EGLN) in individuals with features of phaeochromocytoma and renal cell carcinoma susceptibility. *Endocr. Relat. Cancer* **18,** 73–83
52. Niu, X., Miasnikova, G. Y., Sergueeva, A. I., Polyakova, L. A., Okhotin, D. J., Tuktanov, N. V., Nouraie, M., Ammosova, T., Nekhai, S., and Gordeuk, V. R. (2009) Altered cytokine profiles in patients with *Chuvash polycythemia*. *Am. J. Hematol.* **84,** 74–78
53. Pastore, Y., Jedlickova, K., Guan, Y., Liu, E., Fahner, J., Hasle, H., Prchal, J. F., and Prchal, J. T. (2003) Mutations of von Hippel-Lindau tumor-suppressor gene and congenital polycythemia. *Am. J. Hum. Genet.* **73,** 412–419
54. Ali, N., Karlsson, C., Aspling, M., Hu, G., Hacohen, N., Scadden, D. T., and Larsson, J. (2009) Forward RNAi screens in primary human hematopoietic stem/progenitor cells. *Blood* **113,** 3690–3695
55. Stein, A. A., Schilp, A. O., and Whitfield, R. D. (1960) The histogenesis of hemangioblastoma of the brain: a review of twenty-one cases. *J. Neurosurg.* **17,** 751–761
56. Vortmeyer, A. O., Frank, S., Jeong, S. Y., Yuan, K., Ikejiri, B., Lee, Y. S., Bhowmick, D., Lonser, R. R., Smith, R., Rodgers, G., Oldfield, E. H., and Zhuang, Z. (2003) Developmental arrest of angioblastic lineage initiates tumorigenesis in von Hippel-Lindau disease. *Cancer Res.* **63,** 7051–7055
57. Shively, S. B., Beltaifa, S., Gehrs, B., Duong, H., Smith, J., Edwards, N. A., Lonser, R., Raffeld, M., and Vortmeyer, A. O. (2008) Protracted haemangioblastic proliferation and differentiation in von Hippel-Lindau disease. *J. Pathol.* **216,** 514–520